Thesis

Regional histological and microstructural variation within the uterosacral ligament in context of pelvic floor disfunction

Submitted by

Marco Milcher

in partial fulfillment of the requirements for the degree of

Doktor der gesamten Heilkunde

(Dr. med. univ.)

at the

Medical University of Graz

executed at the

Gottfried Schatz Research Center

at the Division of Macroscopical and Clinical Anatomy

under the supervision of

Univ.- Prof. Dr.med. Niels Hammer

Univ.-Ass. Annika vom Scheidt, PhD

Graz, 24.06.2025

Declaration of Academic Integrity

I hereby confirm that the present diploma thesis is the result of my own independent scholarly work. I also confirm that in all cases, where material from the work of others (in books, articles, essays, dissertations, and on the internet) is acknowledged, quotations and paraphrases are clearly indicated. No material other than that cited in the reference list has been used. I have read and understood the Medical University's regulations and procedures concerning plagiarism.

Furthermore, I hereby declare that if artificial intelligence (AI) tools were used for the generation and/or correction of certain text passages in the creation of this work, such employment was conducted in compliance with ethical principles, academic integrity, and the regulations of my university. Additionally, it was ensured that this usage was transparently disclosed and appropriately attributed.

Graz, 24.06.2025 *Marco Milcher, m.p.*

Acknowledgements

I would like to express my gratitude to Univ.-Prof. Dr. Niels Hammer, Head of the Division of Macroscopic and Clinical Anatomy in Graz, for his invaluable guidance and support throughout my work.

I am especially thankful to Univ.-Ass.in Annika vom Scheidt, PhD., for her exceptional mentorship, insightful feedback, and constant availability as my advisor and key contact person. Her expertise, attention to detail, and dedication were instrumental in shaping the direction and quality of this work. She consistently provided thoughtful suggestions and encouragement, which enhanced both my research and my personal development. Her kindness and approachability created an environment in which I felt supported and inspired.

My deepest thanks go to the entire team at the Division of Macroscopic and Clinical Anatomy, whose expertise and collaborative spirit created an inspiring working environment. I am particularly grateful for the significant support provided during the histological analyses, which was crucial to this project.

Finally, I wish to thank my family and friends for their unwavering support, encouragement, and patience throughout my studies. Their belief in me has been an indispensable source of motivation and strength.

Zusammenfassung

Ziel: Die Ligamenta sacrouterina (uterosacral ligaments, USL) sind wichtige anatomische Strukturen im kleinen Becken der Frau. Sie verlaufen vom kaudalen Teil des Uterus und der Cervix uteri das Rektum lateral umscheidend nach dorsal und verbinden sich fächerförmig im Bereich des Sakrums mit der Fascia endopelvina und im kaudalen Bereich mit den Faszien der Beckenbodenmuskulatur. Aktuelle Forschungsergebnisse weisen darauf hin, dass sich die Mikrostruktur und die mechanischen Eigenschaften der USL sowohl mit dem Alter als auch bei Dysfunktionen des Beckenbodens durch Zugkräfte ändert. Dies soll unter anderem zum Auftreten von Prolapsgeschehen der Beckenorgane (pelvic organ prolapse, POP) beitragen.

Ziel dieser Studie war es, histologische und mikrostrukturelle Unterschiede in verschiedenen Regionen der USL in Abhängigkeit vom Alter zu analysieren. Zudem sollte untersucht werden, inwiefern der in manchen Studien erwähnte „deep layer“ - ein tief verlaufender Teil der USL, welcher in Richtung der Beckenbodenmuskulatur zieht - makroskopisch und histologisch identifizierbar ist.

Methoden: Eine umfassende Literaturrecherche zum aktuellen Forschungsstand über die Funktion und Struktur der USL und der mögliche Zusammenhang mit POP wurde durchgeführt. Bei 23 weiblichen Körperspenden (13 unfixierte, 10 fixierte) wurden die USL zunächst makroskopisch in situ untersucht. Anschließend wurden die rechten USL der unfixierten Spenden entnommen und histologisch mittels Hematoxylin-Eosin-, Siriusrot-, Masson-Goldner-Trichriom- und Resocin-Fuchsin-Färbung gefärbt und analysiert. Bei den fixierten Präparaten erfolgte eine vollständige Präparation in situ und anschließend eine Entnahme und histologische Untersuchung (ebenfalls mittels Hematoxylin-Eosin-, Siriusrot-, Masson-Goldner-Trichriom- und Resocin-Fuchsin-Färbung) der rechten USL.

Ergebnisse: Unsere Studie zeigte eine regionale Heterogenität der USL: Der zervikale Bereich war makroskopisch besonders fest und breit ausgeprägt und zeigte eine starke Verbindung mit der Muskulatur der Cervix uteri. Im sakralen Bereich dünnten sich die USL aus und bestanden im Bereich des Ansatzes am Sakrum zum Großteil aus lockerem Bindegewebe, dass sich fächerförmig aufspannte. Zudem wurde eine Asymmetrie bezüglich der Längen festgestellt, es zeigte sich in allen untersuchten Präparaten das linke USL kürzer als das rechte. Die mikroskopische Untersuchung unter Anwendung verschiedener

Färbetechniken ermöglichte eine detaillierte Analyse der Zusammensetzung des USL, wobei insbesondere regionale Unterschiede in der Ausrichtung der Kollagenfasern sowie in der Verteilung von glatter Muskulatur, Binde- und Fettgewebe sichtbar wurden. Trotz fehlender statistischer Signifikanz aufgrund der kleinen Stichprobe konnte in Bezug auf die Verteilung von glatter Muskulatur ein um bis zu 5-mal höherer Anteil an glatten Muskelfasern in der jungen Gruppe im Vergleich zur gealterten Gruppe festgestellt werden. Ebenfalls konnten visuell deutliche Unterschiede zwischen einzelnen Körperspenden festgestellt werden, was vermutlich auf die hohe interindividuelle Variabilität zurückzuführen ist.

Schlussfolgerung: Die beobachtete interindividuelle Variabilität in der Ausprägung der verschiedenen Komponenten und der unterschiedliche Anteil an glatter Muskulatur in den Altersgruppen sind besonders für die Urogynäkologie relevant. Das erweiterte Wissen über die regionale Struktur und Hinweise auf altersabhängige Veränderungen des USL bringt zusätzliche Informationen zur Weiterentwicklung und Optimierung operativer Verfahren zur Korrektur von POP.

Abstract

Objective: The uterosacral ligaments (USL) are important anatomical structures in the female pelvis. They extend from the caudal part of the uterus and the cervix, running laterally around the rectum, and fan out to connect with the endopelvic fascia at the sacrum and the fascia of the pelvic floor muscles. It is hypothesized that the microstructure and mechanical properties of the USL change with age and in cases of pelvic floor dysfunction due to tensile forces. This may contribute to the development of pelvic organ prolapse (POP).

The aim of this study was to analyze histological and microstructural differences in various regions of the USL. Additionally, we aimed to investigate whether the "deep layer" mentioned in some studies - a deeply running part of the USL extending toward the pelvic floor muscles - can be identified macroscopically and histologically.

Methods: A comprehensive literature review on the current research regarding the function and structure of the USL and their possible association with POP was performed. The USL of 23 female cadavers (13 unembalmed, 10 embalmed) were first examined macroscopically in situ. Subsequently, the right USL of the unembalmed specimen were excised and histologically analyzed using Hematoxylin-Eosin, Sirius Red, Masson-Goldner-Trichrome, and Resorcin-Fuchsin staining. In the fixed specimens, a complete in situ dissection was performed, followed by the extraction and histological examination of the right USL (also using Hematoxylin-Eosin, Sirius Red, Masson-Goldner trichrome and Resorcin-Fuchsin staining).

Results: Our study demonstrated regional heterogeneity within the USL: The cervical region was particularly firm and broad, whereas the USL became less dense and fanned out in the sacral region. Additionally, an asymmetry in length was observed, with the left USL being shorter than the right in all examined specimens. Microscopic examination using various staining techniques enabled a detailed analysis of the composition of the USL, revealing regional differences in the orientation of collagen fibers as well as in the distribution of smooth muscle, connective tissue, and fat tissue. Although statistical significance could not be established due to the small sample size, a distributional difference in smooth muscle showed up to a fivefold higher proportion of smooth muscle in the young group compared to the aged group. Clear visual differences were also observed between individual body donors, which is likely attributable to high interindividual variability.

Conclusion: The observed interindividual variability in the expression of the different components and the varying proportion of smooth muscle across age groups are particularly relevant in the clinical field of urogynecology. The expanded knowledge of the regional structure and indications of age-related changes in the USL provide additional information for the further development and optimization of surgical procedures for the correction of POP.

Contents

List of abbreviations

BL	broad ligament
BMI	Body Mass Index
CI	confidence interval
CL	cardinal ligament
cm	centimeter
HE	hematoxylin and eosin
mm	millimeter
MMP	matrix metalloproteinase
MR	magnetic resonance
MRI	Magnetic Resonance Imaging
PBS	phosphate buffered saline
PC	personal computer
PFMT	pelvic floor muscle training
POP	pelvic organ prolapse
POP-Q	Pelvic Organ Prolapse Quantification
RL	round ligament
SD	standard deviation
TVL	total vaginal length
USL	uterosacral ligament

List of figures

List of tables

1. Introduction

1.1. Relevance

Pelvic organ prolapse (POP) is a very common, benign condition in women. Genital descent refers to the downward displacement of the bladder (cystocele), rectum (rectocele), small and/or large intestine (enterocele), vagina, or uterus (1). The descent of the pelvic organs can lead to symptoms such as vaginal bulge and pressure, voiding dysfunction, defecatory dysfunction, and sexual dysfunction, which may significantly impact the affected women's quality of life (2).

The following chapter will discuss the possible causes of POP, its clinical presentation, diagnosis and staging, as well as potential conservative and surgical treatment options.

The second part of the chapter explains the necessity of this study and provides an overview of the methods used to address the open questions regarding the macro- and microstructure of the uterosacral ligament (USL), because those are often targeted in POP reconstructive surgeries.

1.1.1. Clinical relevance

Female pelvic organ prolapse (POP) is a very common condition of multifactorial genesis. POP is diagnosed when pelvic organs, particularly the internal female genital organs, descend from their normal anatomical position. It is likely that combinations of anatomical, physiological, genetic, lifestyle, and reproductive factors interact throughout a woman’s lifespan to contribute to pelvic floor dysfunction. While many factors play a role in the development of POP, the major risk factors identified include parity, vaginal delivery, age, and BMI (3–5).

About 40-50% of women in the US between the ages of 45 and 85 have objective evidence of POP. Among these women, approximately 12% experience symptoms. These symptoms include urinary incontinence (73%), urinary urgency and/or frequency (86%), voiding dysfunction (34-62%), fecal incontinence (31%) pain and inhibited sexual function (3,6–8). Women with symptoms suffer from physical, but especially emotional distress, including reduced quality of life, reduced body image, anxiety, and depression (3,9,10).

The initial evaluation recommended for women with suspected POP involves a comprehensive overview of medical history, an assessment of symptoms and symptom severity, a physical examination, and a discussion of possible treatment and treatment goals. Among these, symptom assessment is the most critical aspect of evaluating a woman with POP (2).

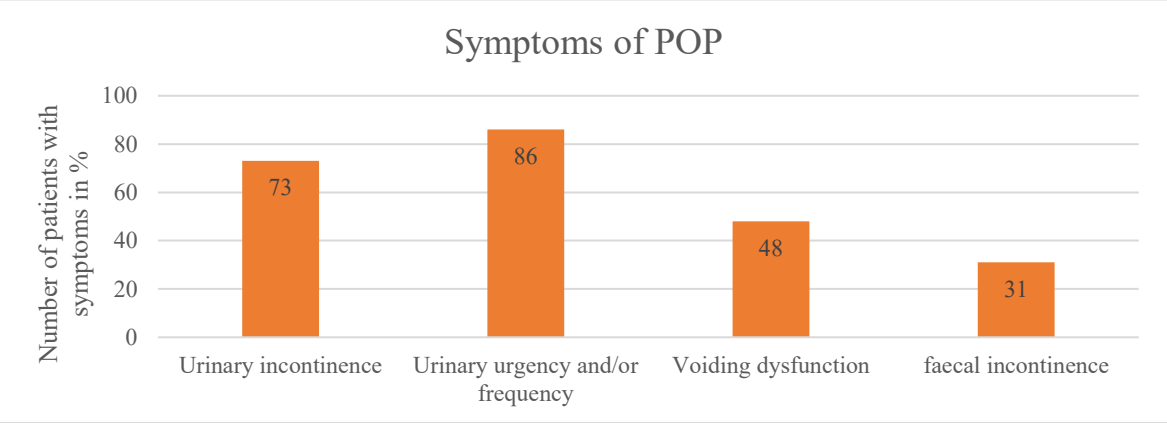

Figure 1: *Symptoms of Pelvic Organ Prolapse according to Ellerkmann et al. (8).*

POP can be divided into different categories based on the severity levels. These levels ranges from Stage 0: no prolapse to Stage IV: complete prolapse (11).

Stage	Characteristics
Stage 0	No prolapse; anterior and posterior points are all −3 cm, and C or D is between −TVL and −(TVL − 2) cm.
Stage I	The criteria for stage 0 are not met, and the most distal prolapse is more than 1 cm above the level of the hymen (less than −1 cm).
Stage II	The most distal prolapse is between 1 cm above and 1 cm below the hymen (at least 1 point is −1, 0, or +1).
Stage III	The most distal prolapse is more than 1 cm below the hymen but no further than 2 cm less than TVL.
Stage IV	Represents complete procidentia or vault eversion; the most distal prolapse protrudes to at least (TVL − 2) cm.

Table 1: *Stages of Pelvic Organ Prolapse, Boyles et al. (11) .*
C, cervix; D, posterior fornix; TVL, total vaginal length.

To standardize the comparison of women with POP, the POP-Q system was established, which allows for the quantification of various manifestations of POP (12). An examination using the POP-Q system should be performed prior to any POP therapy to ensure objective evaluation and documentation of the prolapse. It is a recommended tool by major national and international urogynecologic health organizations, including the American Urogynecologic Society, the Society of Gynecologic Surgeons, and the International Continence Society (7,13).

In this system, nine defined points along the midline of the vagina are measured relative to the hymen of the examined woman. During the examination, the patient performs a maximal Valsalva maneuver (12).

The following points are used for the assessment:

Abbreviation	Description
Aa	3 cm proximal to the external urethral meatus
Ba	most prolapsed portion of the anterior vaginal wall
C	leading edge of the cervix or vaginal cuff
gh	middle of the urethral meatus to the midline of the posterior hymen
pb	middle of the posterior hymen to the middle of the anal opening
tvl	maximum depth of the vagina with prolapse reduced
Ap	3 cm proximal to the posterior hymen
Bp	most prolapsed portion of the posterior vaginal wall
D	posterior fornix in a woman who has a cervix

Table 2: *Pelvic Organ Prolapse Quantification System, AUGS Guidelines (2).*

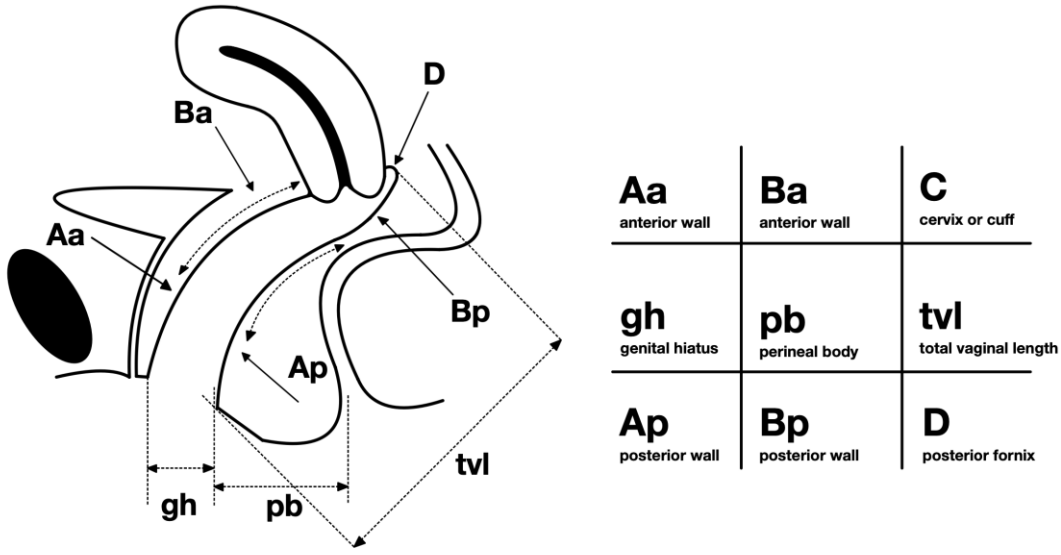

Figure 2: *Pelvic Organ Prolapse Quantification System, AUGS Guidelines (2).*
Created by author using Notability.

There are various options for treating POP. Conservative methods include observation, lifestyle changes, pessary therapy and pelvic floor muscle training (PFMT) (1,14). Six months of supervised PFMT has benefits in terms of anatomical and symptom improvement (urinary incontinence and frequency and bother of other symptoms) (14).

However, since conservative treatments are not always sufficient to alleviate or control the symptoms, several surgical techniques have been established for the treatment of POP. Due to the severity and high number of symptoms, the lifetime risk of surgery for POP in the general female population is 11.1% (3). Surgery is recommended for women who are significantly bothered by their POP and have either failed or declined nonsurgical treatments (1,2).

Key factors in determining the type of surgery include the location and severity of the prolapse, the nature of the symptoms, the patient's overall health, their personal preferences, and the surgeon's expertise (2,15).

According to the guidelines of the German (DGGG), Austrian (OEGGG), and Swiss (SGGG) Societies for Gynecology and Obstetrics, surgical techniques for pelvic organ prolapse are categorized based on the affected pelvic compartment.

If the anterior compartment is affected (bladder = cystocele), treatment options include anterior colporrhaphy (anterior vaginal wall repair) or the insertion of synthetic or biological implants.

If the prolapse involves the posterior compartment (rectum = rectocele, large and/or small intestine = enterocele), posterior colporrhaphy (posterior vaginal wall repair) or correction using synthetic or biological implants are possible approaches.

For prolapse in the middle compartment (vagina, uterus), surgical techniques include abdominal sacrocolpopexy, uterosacral ligament fixation, sacrospinous fixation and uterosacral hysteropexy.

Since this study focuses on the macro- and microstructure of the uterosacral ligament (USL), the following sections will provide a more detailed discussion of surgical treatments for prolapse in the middle compartment:

Abdominal, laparoscopic or robotic-assisted sacrocolpopexy is a well-established and effective surgical option for managing POP in patients that have had a previous hysterectomy. This procedure involves attaching a synthetic mesh or biologic graft from the vaginal apex to the anterior longitudinal ligament of the sacrum. Patients eligible for abdominal sacrocolpopexy include women with a shortened vaginal length, intraabdominal pathology, or factors that increase the risk of recurrent POP, such as being under 60 years of age, having stage III or IV prolapse, or a body mass index exceeding 26 kg/m^2. In women at higher risk of complications related to synthetic mesh (such as those using chronic steroids or who are current smokers) alternatives like sacrocolpopexy with a biologic graft or other surgical approaches may be more suitable (1,2,15).

Vaginal apex suspension is indicated for patients with uterine prolapse, as vaginal hysterectomy alone is insufficient for adequate treatment in such cases. Performing this procedure alongside a hysterectomy helps lower the risk of recurrent POP. Vaginal apex suspension involves securing the vaginal apex to either the uterosacral ligaments (uterosacral ligament suspension) or the sacrospinous ligaments (sacrospinous fixation). Both techniques are equally effective for treating POP and offer similar outcomes in terms of anatomy, functionality, and potential complications (2,15,16).

Uterosacral ligament fixation is performed by attaching the vaginal apex bilaterally to the ipsilateral uterosacral ligament or by attaching the vaginal apex to uterosacral ligament complex that is plicated in the midline (1,2,17). It is important that an adequate segment of uterosacral ligament is secured to the vagina. This often requires attachment to the midportion of the uterosacral ligament close to the ischial spine (9,18).

Sacrospinous fixation can be a suitable alternative. The sacrospinous ligament is used to support the uterus or vaginal apex after hysterectomy. A unilateral right sacrospinous ligament fixation usually is used for the attachment point to avoid dissection around the rectum (1,2,19).

Uterosacral or sacrospinous hysteropexy represents an alternative approach in which, the uterus is preserved and no synthetic mesh or biological graft is needed. The cervix is secured to the uterosacral or sacrospinal ligament. However, there is insufficient data to determine any differences in safety and effectiveness compared to procedures involving hysterectomy (1,20).

Surgical Technique		**Aim**	**Indication**
Abdominal sacral colpopexy		Correct upper vaginal prolapse	Most commonly used in women with recurrent cystocele, vault or enterocele.
Vaginal apex suspension	Uterosacral ligament suspension	Correct upper vaginal prolapse	Performed at the time of hysterectomy or in patients with posthysterectomy vaginal vault prolapse.
	Sacrospinous fixation	Correct upper vaginal prolapse	
Uterosacral or sacrospinous hysteropexy		Correct prolapse and preserve uterus	For younger patients with desire for future pregnancy and patients that require shorter operating time due to health reasons.

Table 3: *Surgical techniques to treat POP.*
German (DGGG), Austrian (OEGGG), and Swiss (SGGG) Societies for Gynecology and Obstetrics (1), AUGS Guidelines (2).

A problem with surgical treatment of POP is that there is often a need for reoperation due to recurrent prolapse. For example, the risk for vaginal prolapse after total hysterectomy and uterosacral ligament suspension is as high as 6 to 12% (6,21). Since the USL consists of connective tissue structures, they can become more stretchable over time and may not provide stable support for the vagina (9,22).

Another issue in evaluating the USL as a potential structure for vaginal support is that in current studies, often only a partial area of the USL is examined and studied, making a comprehensive evaluation of the USL's properties difficult, which will be discussed is more detail in the next section. Additionally, as mentioned above, POP has a multifactorial genesis and it is very challenging to take all different factors into account (3).

1.1.2. Relevance from a fundamental research point of view

In reviewing the existing literature, discrepancies exist between the descriptions of the USL in anatomical studies and surgical-gynecological studies.

In anatomical studies, the USL is described as a delicate structure, especially in the sacral region where it is not well-defined (23). In contrast, surgical studies describe the USL as a dense structure that is easily identifiable during an operation (24,25).

Another necessity for conducting this research project is the limited number of studies that divide the USL into three different regions based on histological characteristics. Many works still refer to the division into three equal parts, as described by Campbell in 1950. However, a study by Vu et al. demonstrated that the histological differences in the regions do not correspond to equal thirds (9,23–27).

Furthermore, current research lacks studies that examine the histology of the deep part of the USL. This part of the USL is mentioned in the macro-anatomical studies by Vu (24) and Iwanaga (26), as well as in the study by Umek (28) using MRI. It is described that this deep part of the USL has connections to the pelvic floor muscle fascia, particularly the fascia of the coccygeus muscle and the sacrospinous ligament.

This highlights the importance to describe the USL as an anatomical structure macroscopically and to investigate it histologically in all regions and levels.

A major issue in reviewing studies that examined the USL is that most studies did not describe how samples were taken. Due to the lack of an existing standardized sampling

method, we had to develop our own methods to generate representative and reproducibly positioned samples.

1.2. Ligaments of the uterus

The subperitoneal pelvic connective tissue consists of heterogenous, fibrous reinforcement, which have been collectively referred to as the Corpus intrapelvinum (29). From the central parts of the Corpus intrapelvinum, pillars extend to various organs, reaching the bladder as the paracystium (anterior pillar), the vagina and the uterus as the paracolpium and the parametrium (middle pillar), and the rectum as the paraproctium (posterior pillar). Pathological processes, which are linked to the course of blood and lymphatic vessels, therefore spread within the Corpus intrapelvinum (29,30).

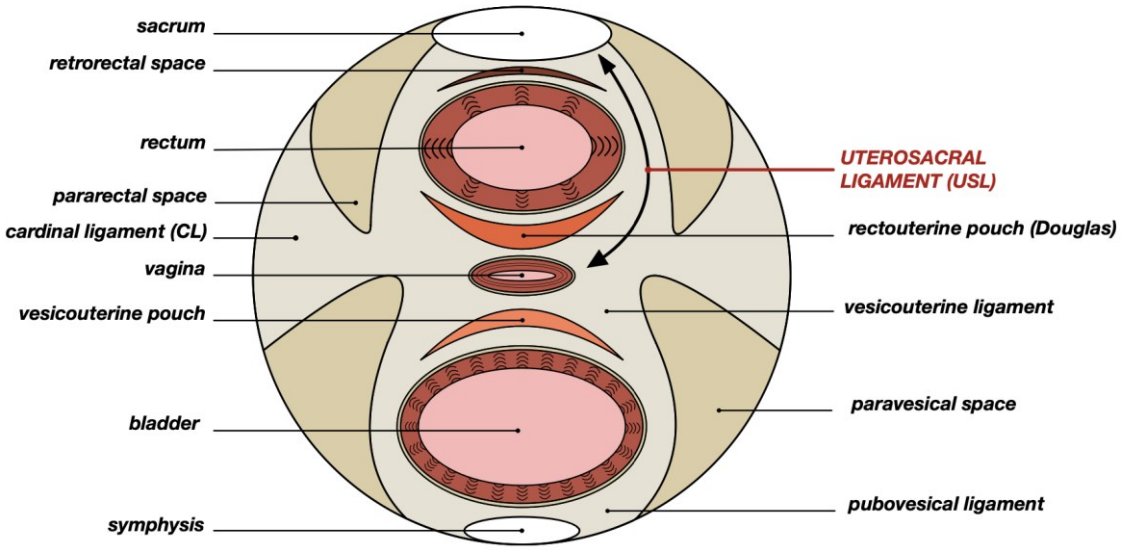

Figure 3: *Scheme of organs, spaces and ligaments in female pelvis, cross section. Created by author using Notability.*

The individual bands of the Corpus intrapelvinum are not uniformly structured. They contain varying amounts of collagen, elastin, smooth muscle tissue, blood vessels, lymphatic structures, fat, and parasympathetic nerves (9). There are several structures of connective tissues, referred to as “ligaments” or “bands”. The ones supporting the position of the uterus are described as cardinal ligament, the broad ligament, the round ligament and the uterosacral ligament.

The cardinal ligament (CL, Ligamentum cardinale, Ligamentum transversum cervicis Mackenroth) is a part of the parametrium. It originates broadly at the lateral pelvic wall and extends towards the uterus and superior part of the vagina. Before reaching these two organs, the CL branches ventrally into the paracystium and dorsally into the paraproctium. It then reaches the cervix uteri as the paracervix and the vagina as the paracolpium (30).

The broad ligament (BL, Ligamentum latum uteri) consists of a double layer of peritoneum that stretches from the sides of the uterus to the pelvic wall. Often termed the "female genital mesentery", the BL and the uterus effectively split the pelvic cavity into two separate compartments: the recto-uterine pouch, located between the uterus, rectum, and parts of the sigmoid colon, and the vesico-uterine pouch, positioned between the uterus and the bladder. The superior part of the BL divides into the mesosalpinx and mesovarium. These structures are described as support tissues for the fallopian tube and the ovary (18).

The round ligament (RL, Ligamentum teres uteri, ligamentum rotundum) originates from the tubal angle on each side. In a peritoneal fold in reaches the internal inguinal ring, and passes through the inguinal canal. The fibers of the round ligament then extend into the connective tissue of the mons pubis and the labia majora (30).

The uterosacral ligament (USL, Ligamentum sacrouterinum) connects the cervix towards the rectum and the sacrum. This ligament creates a distinct peritoneal fold (the rectouterine fold, Plica rectouterina), which forms the upper boundary of the pouch of Douglas. The uterosacral ligament is the main component of the paraproctium (9,23,30).

1.2.1. Function of the uterine ligaments

The position and movement of pelvic organs are determined by the interaction of several structures, predominantly the muscles of the pelvic floor and the uterine ligaments. The function of these structures can be simplified by envisioning a boat in a dock. The boat itself represents the uterus. The water represents the pelvic floor muscles, while the ropes securing the boat represent the uterine ligaments. These components work together to secure the position of the uterus and restrict its mobility within the pelvis.

When the water level in the doc drops, more tension is exerted on the ropes, which can become stretched and damaged over time. Similarly, damage or insufficiency of the pelvic

floor results in increased tension on the uterine ligaments. This leads to increased stretching and may result in uterine malposition and furthermore in pelvic organ prolapse (22,23).

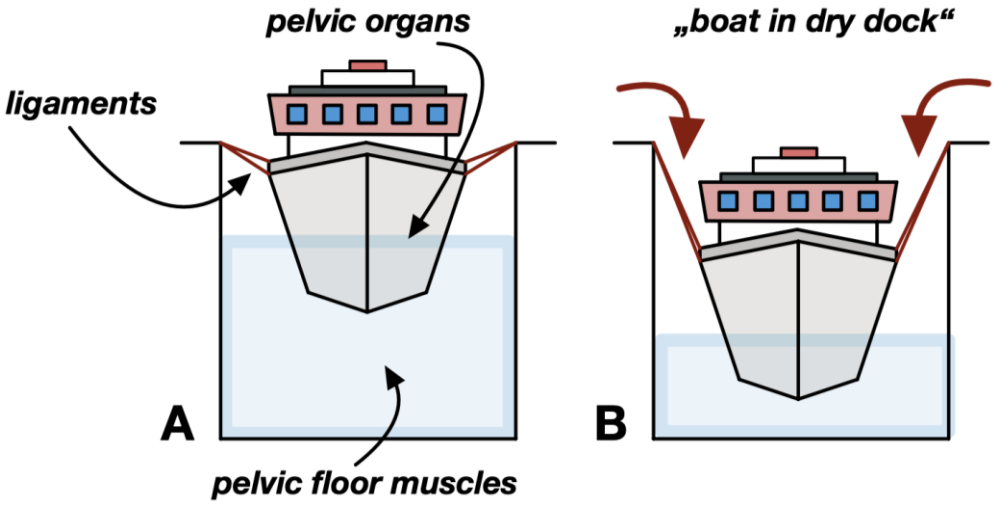

Figure 4: *“Boat in dock” analogy introduced by Norton (22).*
A: *The boat represents the pelvic organs, the ropes holding the boat represent the ligaments that support the organs and the water represents the pelvic floor muscles.*
B: *If the water level drops, the boat (organs) hangs on the ropes (ligaments). The ropes stretch out and break, resulting in the boat (organs) to drop lower (i.e., pelvic organ prolapse (POP)).*
Created by author using Notability.

Another hypothesis is that a change of the composition of the pelvic floor ligaments and fascia is a cause of pelvic support disorders. Collagen and elastin provide the strength and flexibility of these structures (22) and can be effected by aging (27).

During pregnancy, the uterine ligaments allow for the expansion of the uterus. Through growth and increased muscularization, these supportive bands become strong, rope-like structures that pull downward from the uterus to their anchor points. During strong uterine contractions (labor pains), these bands act as a counterbearing and provide support for the uterus, pushing the child downward through the birth canal (30).

1.3. Uterosacral ligament (USL)

1.3.1. Gross anatomy

The uterosacral ligament (USL, Ligamentum sacrouterinum) is an essential part of the paraproctium, which dorsally connects the cervix and superior part of the vagina to the

rectum and sacrum. This ligament forms a distinct peritoneal fold (Plica rectouterina) and forms the upper margin of the Excavatio rectouterina (rectouterine pouch, Douglas pouch) (30).

Although there has been increased research on the USL in recent years, most studies still refer to Campbell's anatomical description from 1950 (23).

Campbell describes the USL as fan-shaped structures with a membranous quality. They extend between the sacrum and the posterior-lateral cervix and apical vagina in an angle slightly greater than 90° from the body`s cephalic-caudal body axis, thereby encircling the rectum (9,23).

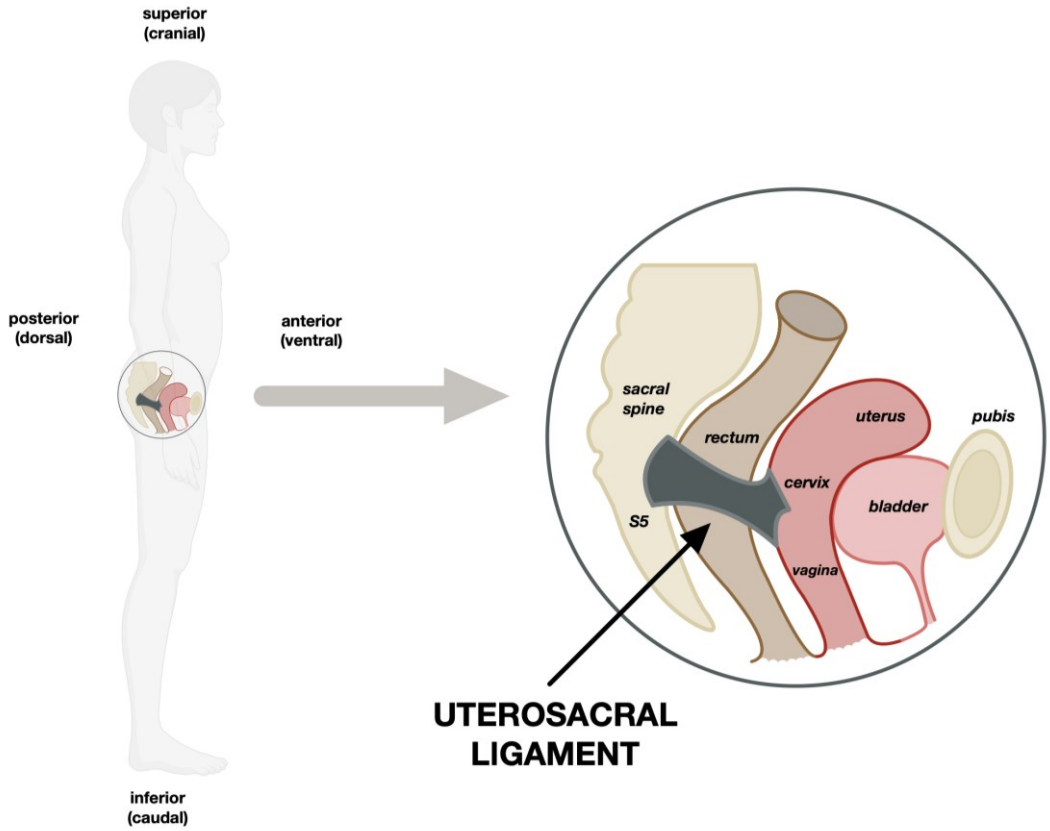

Figure 5: *Anatomic orientations and directions and right USL within the female pelvis. Created by author using Notability.*

While the USL manifest as distinct bands of peritoneum-covered tissue near the cervix, they become thinner and less distinctly apparent as they progress posteriorly (9,23).

Due to the anatomical position of the sigmoid colon and cranial portion of the rectum on the left side of the pelvis and the continuous covering of peritoneum over the USL and the

rectum, the left USL generally appears less developed than the right. When traction is applied to the uterus moving it ventrally, the right USL or the rectouterine fold appears more prominent (23,24), which is used during surgery to identify the USL (24).

Rich blood supply is evident at the cervical end of the ligaments, primarily deriving from branches of the uterine vessels. Vessels become fewer and smaller in the middle part of the and are reduced numbers in the sacral part (9,23).

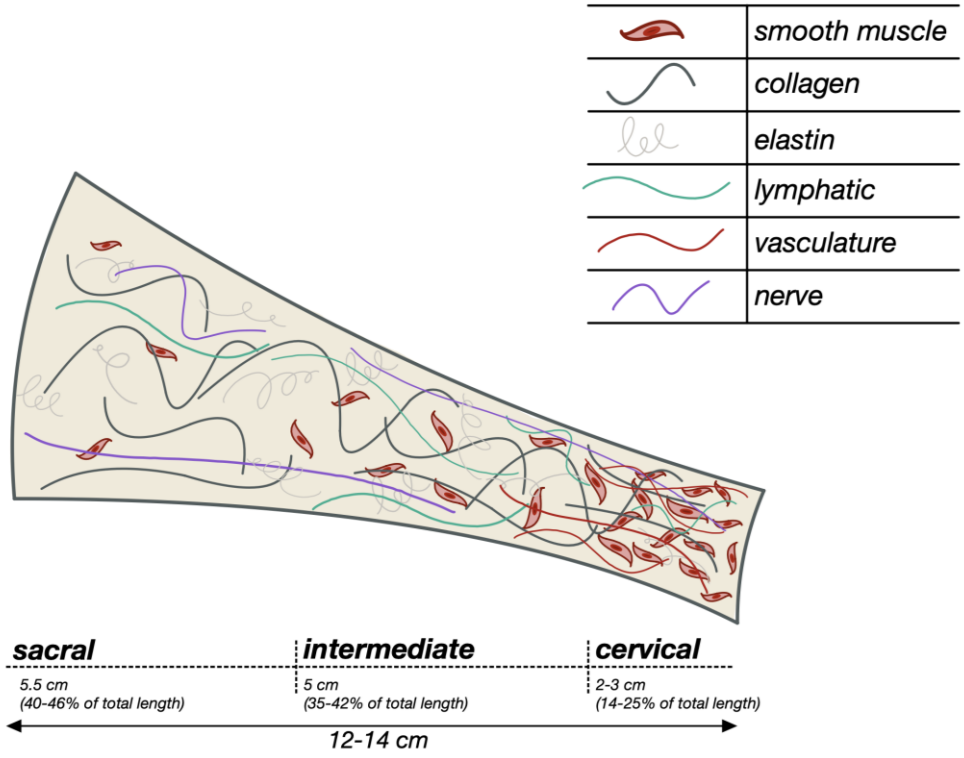

Figure 6: *Distribution of different tissue and cells in the USL.*
Cervical, intermediate and sacral regions, main microstructural components, and ranges of length of the USL.
Created by author using Notability.

Nerve components within these ligaments are challenging to identify macroscopically. Parasympathetic nerve fibers from sacral segments two, three, and four can be identified in the intermediate and anterior thirds of the ligaments, forming the parasympathetic autonomic innervation of the uterus. Sympathetic fibers, accompanying the uterine artery, contribute to the sympathetic autonomic innervation of the uterus (9,23,24).

Additionally, lymphatic vessels within these ligaments drain the cervix and lower uterine body toward the sacral nodes and onwards to the common iliac and perilumbar nodes (23).

1.3.2. Function

By virtue of their location, course, attachment, and reported fibromuscular components, the uterosacral ligaments should be an important factor in maintaining the elevation and posterior orientation of the uterus and cervix (28).

1.3.3. Insertion points

When examining the insertion points of the USL, a distinction must be made between the distal origin at the genial organs (uterus, cervix, and vagina) and the proximal attachment in the sacral region.

Cervical attachment

Regarding the insertion around the genital organs most authors present similar findings. They describe the insertion points at the posterolateral part of the cervix near the internal os and the apical vagina (23–25,28).

Campbell and Buller additionally describe an interweaving of the fibers of the USL with those of the cardinal ligament (CL) in the region of the cervix (23,25).

In a study by Umek, a differentiation was made regarding the exact location of the insertion at the genital organs. In all the women examined (82), 254 individual distal insertion points were found. Of these, 84 (33%) had connections to the cervix, 161 (63%) showed a common insertion in the area of the cervix and vagina, based on an MR imaging. In 9 cases (4%) there was a connection to the vagina below the cervix (28).

Sacral attachment

There is a greater discrepancy when considering the proximal insertion points of the USL in the sacral region.

Most investigators agree that the proximal insertion of the USL occurs at the height of the S2 to S4 segments of the sacral spine (9,31).

Both anatomical studies and studies using MRI studies suggest there is an additional, deeper insertion (deep layer of USL) towards the pelvic floor. This includes insertion points at the sacrospinous ligament and the coccygeus muscle (23,25,28,32).

In a macro-anatomical study with 33 cadavers, Campbell describes an insertion of the proximal fibers close to the S2 to S4 segments of the sacrum in the area of the sacroiliac joint and the lateral edge of the sacrum (23).

In a similar macro-anatomical cadaveric study with 11 individuals, Buller et al. describe a predominant number of insertion points around the S1 to S3 segments of the sacrum, with a variable extension caudally to the S4 segment. Additionally, fibers were described that extend towards the sacrospinous ligament and form connections there (25).

Both authors emphasize, that the attachment does not occur directly to the sacral bone, but is mediated via the endopelvic fascia and the periosteum of the sacrum (23,25).

In an anatomical MR study by Umek et al. with 82 individuals, 259 individual insertion points on the pelvic sidewall were found. An insertion at the sacrum was described in only 7% (19) of the cases. Instead, in 82% (213) of the examined cases, a proximal insertion of the fibers was found to connect to the sacrospinous ligament and the coccygeus muscle. In 11% (27) of the cases, a connection to the piriformis muscle, the area of the sciatic foramen, or the ischial spine was shown (28).

Fritsch also came to a similar result. In this study, which investigated the sectional anatomy of fetal and adult pelves by computed tomography and magnetic resonance imaging, no direct insertion point of the uterosacral ligament with the sacrum was demonstrated (33).

This creates further evidence that the uterosacral ligaments rather connect to structures ventral or lateral to the sacral bone than to the bone itself.

According to a review by Vu, these different findings could be due to the definition of the USL. If the ligament is equated with the rectouterine fold, the insertion point is found more cranially in the area of the S1 segment. If the ligament is seen as part of the endopelvic fascia, its insertion is described as consistently broader (24).

Another reason for the different results could be a different understanding of the term "ligament." Depending on how much connective tissue is required and what proportion of certain fibers (collagen, elastin) is needed to define a ligament, different descriptions of the insertion points are obtained (24).

The differing results of the aforementioned studies, especially when comparing macroanatomical and imaging studies, highlight the need for a more detailed investigation of the sacral insertion points, taking into account the already known data.

1.3.4. Measurement methods

The topology and morphometry of the USL is described using different measuring methods in the various studies. Siddique, Buller, and Vu conducted macroscopic measurements on cadavers, while Umek performed measurements using MRI images.

Siddique reports a mean length of the ligament of 8.7 cm from the cervix to its origin at the sacrum along its superior-lateral edge (34).

Vu conducted measurements in both length and width across different regions. The total length of the USL ranged from 12 to 14 cm. The width in the sacral part was reported to be 5 to 20 mm, in the intermediate part 5 mm, and in the cervical part with a variable thickness (24).

According to Buller, the mean width of the uterosacral ligament was 5.2 cm (SD ± 0.9 cm) in the sacral portion, 2.7 cm (SD ± 1.0 cm) in the intermediate portion, and 2.0 cm (SD ± 0.5 cm) in the cervical portion (25).

Umek performed measurements using MR images. The mean length of the uterosacral ligaments in their craniocaudal extent was 21 mm (SD ± 8 mm), calculated from the number of MR images between the most cranial and most caudal image with identifiable origin and insertion points (28).

Furthermore, differences in the measurement methods used in the various studies can be noted. For example, in the study by Umek, the distance (in millimeters) from the midline of the sacrum to the medial border of the ischial bone and from the midline to the insertion point were measured (28). In contrast, in the study by Buller, measurements were taken curvilinearly along the course of the USL (25).

Since the various studies have each focused on certain measurable parameters (e.g., length, width), it would be important to conduct a study that considers all the mentioned parameters. This would allow for better comparability of the results.

1.3.5. Anatomical relationships

Notable anatomical structures that have a close spatial relationship to the USL are the ureters and the nerve roots of the sacral nerves S2, S3, and S4. In some studies, the pudendal nerve is also mentioned, but it was shown that this nerve is located outside the area typically involved in surgeries such as the uterosacral ligament suspension (24,34).

Ureter

The pelvic section of the ureter begins at the Linea terminalis and enters the small pelvis at the bifurcation of the common iliac artery. It crosses the uterine artery at the base of the broad ligament and extends anteriorly along the lateral pelvic wall, ending at the dorsolateral wall of the bladder (24,30).

The distance of the ureter to the insertion point of the USL at the cervix is specified as 2-3 cm (24).

Sacral Plexus

In the area of the sacral origin of the USL, the trunks of the spinal nerves S2, S3, and S4 are in close proximity.

The S1 trunk is usually located cranially to the middle section of the USL and is described as easily identifiable. On average, it is located 3.9 cm (95% CI, 2.1–5.0 cm) cranial to the ischial spine. The S2-S4 trunks cross the USL caudal to its axis. The S2 trunk crosses the USL approximately 2.6 cm, the S3 trunk 1.5 cm and the S4 trunk 0.9 cm cranial to the ischial spine (34).

The close spatial relationship to the adjacent trunks of the sacral plexus is particularly relevant in uterosacral ligament suspension, a surgical option for treating prolapse of the internal female genital organs. It has been shown that especially the trunks of segments S2, S3, and S4 can be directly injured by sutures placed too deeply. Postoperatively, an injury of the described nerves can manifest in patients as neuropathic pain and sensory deficits in the S1–S4 dermatomes, as well as motor deficits (weakness in hip extension and abduction, knee flexion, and plantar flexion). However, due to the variability in plexus formation, no specific symptoms can be identified. Additionally, no precise numbers regarding the incidence of such an injury could be provided (34).

Arteries and Veins

The vessels in the area of the USL appear to course more laterally than the neural structures. In particular, the middle rectal artery, branching from the common iliac artery, is described as potentially at risk during prolapse surgery. This artery reaches the rectum in the sacral region of the USL, embedded in connective tissue (24).

1.3.6. Histology

The histology of the USL is not uniform throughout its entirety. The composition of its components varies by region. Most studies investigating the histology of the USL have divided it into three equal parts: a distal or cervical third, an intermediate third, and a proximal or sacral third (25,26,32). Although it is known, that the distribution of different tissues varies by region, we only found studies that describe the percentual content of smooth muscle, collagen, elastin and fat tissue for the entire USL (9).

The division in different regions was used by Campbell in 1950 to describe the histology of different parts of the USL. Much of the current literature also employs this division for histological descriptions of the USL.

Recent studies done by Buller et al. and Iwanaga et al. have results that align with Campbell's descriptions (25,26):

Distal or cervical third: This section primarily contains densely packed bundles of smooth muscle, which continuously integrate with the smooth muscle of the uterus interwoven with a network connective tissue. Medium and small blood vessels and small nerve bundles are also found in this section (9,23,25,26). There are no studies that describe the specific percentual amount of collagen or elastin in the cervical region.

Intermediate third: The amount of smooth muscle is decreased compared to the cervical third. Also, the prominent blood vessels of the cervical part gradually decrease. In contrast, the amount of connective tissue increases and becomes the main component of the USL in this region. Nerve fibers that are grouped into small bundles in the cervical third aggregate into larger bundles. Parasympathetic ganglia are also found (23,25,26).

Proximal or sacral third: This section consists almost entirely of loose connective tissue bundles interspersed with adipose tissue. Few blood vessels, nerves, and lymphatic tissues are presented (23,25,26).

In contrast to this equal division, some studies focus on the histological components of specific regions. Although the transitions between these regions are gradual, Vu et al. describe the division of the three regions as follows: Out of the average 12-14 cm length of the USL, approximately 2-3 cm (roughly 14–25% of the total length) correspond to the cervical region. The intermediate region accounts for the next 5 cm (roughly 35-42%). The sacral region makes up the remaining 5.5 cm (roughly 40–46% (24).

Regardless of the regional division used, the studies mentioned above focus on the superficial part of the USL, the part that raises the rectouterine fold and is easily identifiable during surgery when the uterus is pulled ventrally. However, authors as Campbell, Buller and Umek also describe macroscopic connections to deeper structures such as the sacrospinous ligament or the coccygeus muscle (25,28,32). Previous to the study at hand, this deep part of the USL has not been described histologically in the literature known to us.

Currently, we are not aware of any studies that have specifically examined the microstructure of the USL in relation to a woman's age.

The study by Campbell (23) describes a case of a 22-year-old woman in which the USL was analyzed in different planes and using various staining techniques. However, this study does not include a comparison with older women.

In the study by Cole (27), the need for a comparison of the USL in women of different ages is mentioned, but no such comparison was conducted in this work either.

1.3.7. Compositional changes of the USL with POP

Pelvic organ prolapse (POP) is associated with microstructural changes in the uterosacral ligaments (USL), particularly involving alterations in collagen, elastin, and other extracellular matrix components (9).

The changes in collagen primarily affect the sub types collagen type I and collagen type III. They seem to be crucial for the ligaments' strength and elasticity. Several studies have found that the collagen type I content in the USL of POP patients is decreased compared to healthy controls (35–39) though some studies have found no change in collagen type I levels (40).

Data on collagen type III is more inconsistent, with some studies reporting a decrease (Connell, Han, Liu), others reporting an increase (Gabriel, Yucel), and still others finding no change in collagen type III levels (39,41).

The regulation of collagen metabolism is also of special interest, particularly the role of matrix metalloproteinases (MMPs) 1, 2, and 9. These enzymes degrade collagen. Many studies report upregulation of MMP-1, MMP-2, and MMP-9, and their respective genes in patients with POP, though some studies report no differences in MMP levels (9,39,42,43).

Elastin is another structural protein crucial for the reversible extensibility of healthy USL. A decline has been linked to POP, although some studies report no significant differences in elastin levels between POP and non-POP groups (9,42,44).

The role of smooth muscle in the supportive function of the USL is less clear but reduced smooth muscle content has been associated with POP. However, some studies have found no differences in smooth muscle content, although structural defects in the smooth muscle of POP patients' USL have been noted (9).

1.4. Aim of this study

The aim of this study is to investigate the USL in its entirety including superficial and deep regions and thereby provide macro- and microanatomical information.

Macroscopic anatomical dissection of fixated specimens allows for a precise and detailed overview of the anatomical relationships, insertion points, and spatial relations to other structures in the female pelvis. By documenting the dissected structures through photographs and detailed descriptions, the results can be presented clearly and made reproducible. Additionally, by measuring the USL before and after dissection, comparisons can be made between the left and right USL as well as between the anatomical position and extent of the Plica rectouterina and the actual USL.

By dissecting unfixed specimen and isolating the USL, samples from the different regions (cervical, intermediate, sacral) and various layers (superficial, intermediate, deep) were obtained and used for histological analysis.

Through the standardized sampling of the predefined regions and histological processing using various staining techniques (Hematoxylin and Eosin, Sirius Red, Masson-Goldner-Trichrome, and Resorcin-Fuchsin staining), different tissue types can be differentiated and the composition of the defined regions can be quantified and compared. Furthermore, by analyzing the samples with image processing software, the orientation of collagen can be

examined and quantified. This allows conclusions to be drawn about the heterogeneous microstructure of the USL.

Through comprehensive research and the various described methods, a holistic picture of the USL's distinct anatomy, histology and its changes throughout life is intended to emerge, providing clinicians with new insights into the macroscopic and histological characteristics, course, length, and insertion points.

2. Materials and methods

This study was conducted on 24 female body donors, comprising 10 embalmed and 13 unembalmed specimens. At first, detailed examinations and measurements of the macroscopic anatomical features were carried out with the embalmed cadavers. The USL of 5 specimen were then dissected and measurements were repeated. Then the USL of 3 specimen were extracted for histological investigation. The USL of the unembalmed body donors were dissected and extracted directly after macroscopic examination and the retrieved samples were deep-frozen at -80°C.

The extracted ligaments underwent comprehensive histological processing. Samples from various regions were prepared and subjected to three different staining techniques to highlight distinct structural components. The stained samples were then evaluated microscopically, with images and measurements obtained using FIJI ImageJ software (45).

The microscopic analysis focused on comparing the microstructural composition of the USL across the different anatomical regions. These included assessments of collagen and elastin arrangement, cellular distribution, and any region-specific variations in tissue architecture.

These comparative evaluations provided insights into the structural heterogeneity of the USL, potentially contributing to a deeper understanding of their functional anatomy.

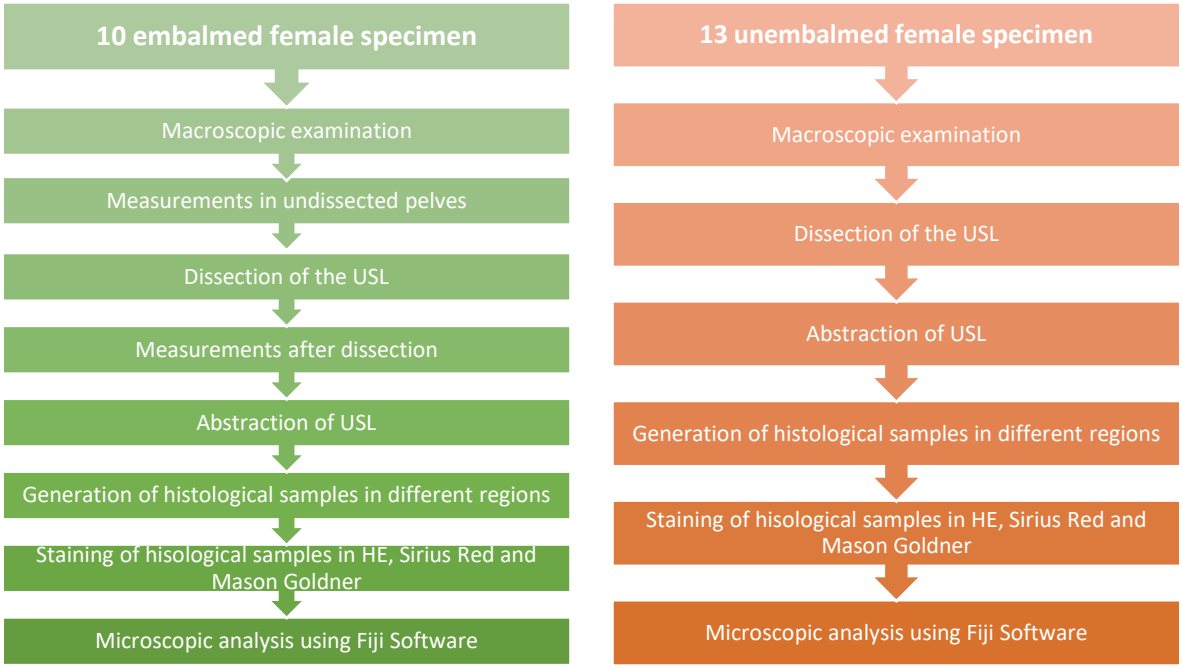

Figure 7: *Methods Overview for embalmed and unembalmed specimen.*

2.1. Literature research

At the beginning of the project, a literature search was performed using the keywords “uterosacral ligament”, “Ligamentum sacrouterinum”, “USL”, “Plica rectouterina”, “pelvic organ prolapse”, and “POP” in the PubMed database. Studies that were not found using the keywords above but were important for our investigation were identified through references cited in other articles. Additionally, anatomy textbooks were searched for descriptions of the USL and pelvic connective tissue.

2.2. Ethical approval

The study was approved by the local institutional review board (#34-49ex21/22). Additionally, all body donors had provided written informed consent during their lifetime at the Division of Macroscopic and Clinical Anatomy, allowing tissue to be used after death for research purposes. In addition, the study was approved by the ethics board of the University Medical Center Hamburg-Eppendorf (#2021-300029-WF), where a small subset of samples was obtained.

The Division of Macroscopic and Clinical Anatomy informs interested persons during their lifetime about the conditions of body donation in accordance with its guidelines. All body donations were pseudonymized in advance with a code number. The data to be evaluated are stored in an Excel spreadsheet on a restricted-access PC. Only authorized persons involved in the study had access to the original data.

2.3. Macroscopy of embalmed pelves

For the macroscopic assessment of the USL, 10 embalmed female cadavers with no evidence of pelvic surgery were examined. Medical, surgical, and obstetric histories were not available. All subjects were adult Caucasians. The average age was 84 years with a range of 71 to 103 years.

2.3.1. Gross anatomy of undissected embalmed pelves

To assess the anatomy of the USL, female specimens were examined as part of the course “Anatomie der Eingeweide und Leitungsbahnen“ at the Medical University of Graz, where they were made available for dissection by students and teaching staff.

Initially, the specimen were inspected for visible scars in the abdominal region to rule out prior surgeries. Additionally, a vaginal palpation was performed to determine the presence of the cervix and uterus.

In total, 10 specimens were selected for macroscopic evaluation. The abdominal wall was opened, and the conditions in the small pelvis were studied and documented in writing and by photography. Additionally, specific conditions such as the position of the uterus, the size of the rectum, or the occurrence of adhesions were noted.

2.3.2. Measurements of undissected embalmed pelves

Measurements were taken in the undissected small pelvis using a flexible ruler. Readings were recorded to the nearest 0.1 cm. The measurements included the anatomical pelvic dimensions as well as the extent of the rectouterine fold in length and width.

These measurements were first taken without applying tension to the uterus. Following that, tension was applied ventrally on the uterus to accentuate the plica rectouterina, and the measurements were repeated. These findings were documented in writing and by photography.

Following measurements were taken (29):

- **Distantia interspinosa:** distance between right and left anterior superior iliac spine..
- **Distantia intercristalis:** widest distance between the iliac crests.
- **Diameter transversa:** maximum transverse distance of the pelvic inlet.
- **Conjugata anatomica:** distance between the upper edge of the pubic symphysis and the promontory.
- **Conjugata vera:** distance between the thickest part of the pubic symphysis and the promontory.

Measurements of undissected embalmed pelves
Outer pelvic measurements
Distantia interspinosa
Distantia intercristalis

Inner pelvic measurements				
Diameter transversa				
Conjugata anatomica				
Conjugata vera				
Uterosacral ligament				
Length curvilinear	Without traction		With traction applied to the uterus	
	Left	Right	Left	Right
Distance between sacrum and cervix				
Width at sacrum	Left		Right	
Width at cervix	Left		Right	

Table 4: *Measurements of undissected pelves.*

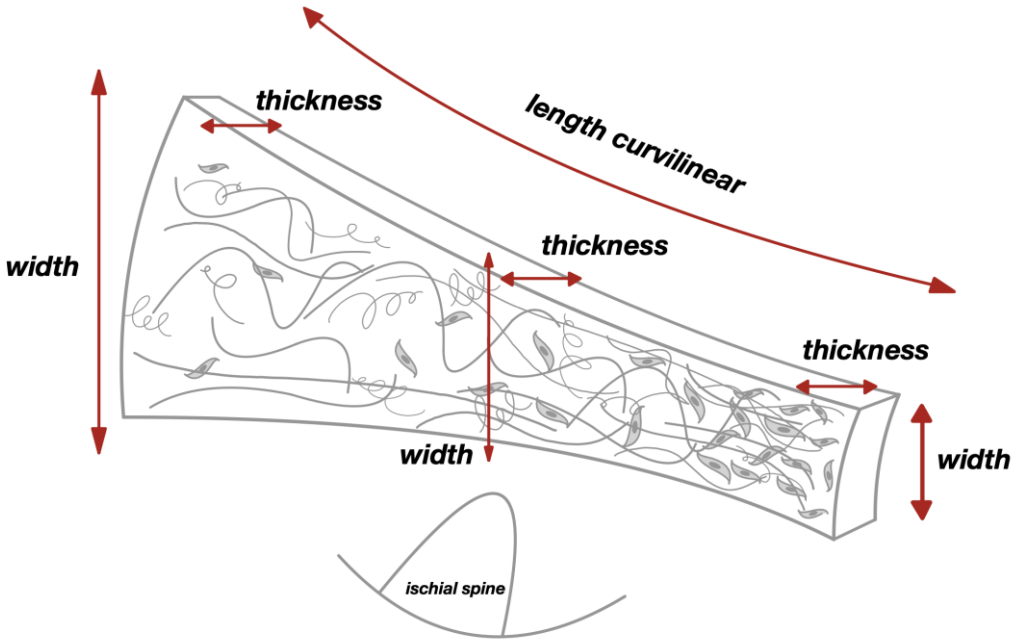

Figure 8: *Measurements of the USL.*
Created by author using Notability.

2.3.3. Gross anatomy of dissected embalmed pelves

In the further course, the pelves of five of these embalmed female body donors were dissected. The course of the USL was identified by locating the plica rectouterina or visible fibers between the sacrum and cervix. Then, starting from the median, the peritoneum was dissected laterally to the pelvic wall, thus exposing the structures of the Plica rectouterina. Care was taken to work very precisely and carefully to avoid damaging the connective tissue and embedded structures. The USL was identified, and its appearance, attachments, and relationships with surrounding structures were documented. Aspects of macroscopic assessment included existence and size of connective tissue fibers, visible nervous fibers and perceptibility of cervical and sacral attachment and deep layer of the USL.

Subsequently, in three of these pelves, the pelvic organs, including the connective tissue structures, were mobilized from the left pelvic wall, and a sagittal division into two hemipelves was performed. Through this division, the dissection of the deep portion of the USL could be performed in the right hemipelvis. This was also documented in writing and by photography. Due to the fact that the examined body donations were included in the anatomy course for medical students at the Medical University of Graz, only 3 of the original 5 specimens were available for detailed preparation.

Aspects of macroscopic assessment		
Connective tissue fibers		
Fibers visible	Yes	No
Size of fibers	Large (>1 mm)	Small (<1mm)
Nervous fibers		
Nervous fibers visible	Yes	No
Insertion points		
Cervical inserting points visible	Yes	No
Sacral inserting points visible	Yes	No
Deep layer and insertion points at pelvic floor visible	Yes	No

Table 5: *Aspects of macroscopic assessment.*

2.3.4. Measurements of dissected embalmed pelves

After the dissection, following measurements were taken:

Measurements of dissected embalmed pelves	
Uterosacral ligament right	
Length curvilinear	
Distance between sacrum and cervix	
Width	at sacrum
	at ischial spine
	at cervix
Depth	at sacrum
	at ischial spine
	at cervix

***Table 6**: Measurements of dissected embalmed pelves.*

2.4. Macroscopy of unembalmed pelves

For the histological assessment of the USL, 13 fresh female cadavers with no evidence of pelvic surgery were examined. All subjects were adult Caucasians. Medical, surgical, and obstetric histories were not available. The average age at the time of death was 69 years, with a range of 29 to 87 years.

2.4.1. Dissection of unembalmed pelves

Before opening the abdomen, a vaginal examination was performed to check whether the cervix was palpable. If the cervix could not be palpated, the body donor was excluded, as a hysterectomy or other surgeries in the pelvic region were highly likely.

If the cervix was palpable, a modified POP-Q score method (Chapter 1.1.1.) was applied to determine a possible post-mortem prolapse. For this, the distance between the cervix and the hymen was measured once in a relaxed and unmanipulated state.

Subsequently, a horizontal traction force of 500g was applied using a clamp attached to the cervix and a spring scale, and the distance was measured again.

Since little information was available in the literature on the exact procedures for dissection and extraction of the USL, we evaluated different approaches to present and extract the ligament in its entirety.

In practice, the optimal approach was first to make a median incision and mobilize the overlying peritoneum from medial to lateral to the pelvic wall. Subsequently, the USL was identified by locating fibers between the sacrum and cervix. The sacral attachment was marked with surgical thread. Then the cervix and the caudal part of the uterus were transected in the median to avoid damaging the distal attachment of the USL.

The USL was mobilized from cranial and lateral as gently as possible and removed in its entirety. Care was taken to cut medially to the major vessels of the internal iliac artery and vein and the ureter. Efforts were made to mobilize the USL as deeply as possible at the pelvic floor to preserve the fibers radiating into the fascia of the levator ani and coccygeus muscles.

The extracted USL were deep-frozen at -80°C and stored until histological processing.

2.5. Histology of embalmed and unembalmed peles

From the three embalmed and 13 unembalmed right USL, 8x6x2 mm cubes were collected as samples for histological examination. The USL was divided into three regions. Two samples were taken from each region: one from the superficial part and another from the deep part. In the sacral region, an intermediate sample was also taken if sufficient material was available.

We decided to divide the USL according to the study of Vu et al. They describe the division of the three regions as follows: Out of the average 12-14 cm length of the USL, approximately 2-3 cm (roughly 14–25% of the total length) correspond to the cervical region. The intermediate region accounts for the next 5 cm (roughly 35-42%). The sacral region makes up the remaining 5.5 cm (roughly 40–46% (24).

The following description should help to simplify orientation:

- **Sample:** Tissue sample taken from the USL
- **Subregion:** Specific localization of the sample within the USL
    - Cervical
        - cervical superficial **(Csup)**
        - cervical deep **(Cprof)** (note: prof. refers to the latin word profund)
    - Intermediate
        - intermediate superficial **(Isup)**
        - intermediate deep **(Iprof)** (note: prof. refers to the latin word profund)
    - Sacral
        - sacral superficial (**Ssup)**
        - sacral intermediate **(Sint)**
        - sacral deep **(Sprof)** (note: prof. refers to the latin word profund)
- **Region:** Grouping of subregions within one section of the USL
    - Csup + Cprof = **Cervical region**
    - Isup + Iprof = **Intermediate region**
    - Ssup + Sint + Sprof = **Sacral region**

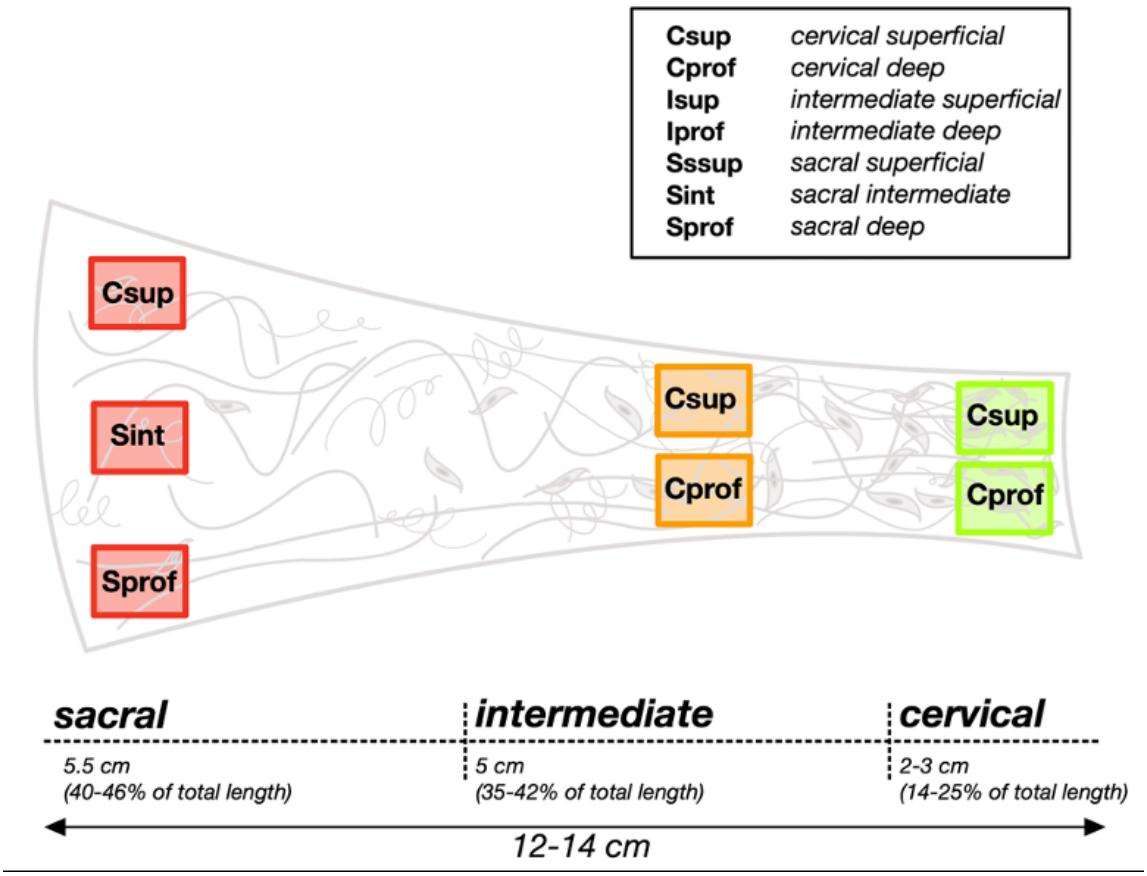

Figure 9: *Division of USL in cervical, intermediate and sacral section.*
Created by author using Notability.

After extraction, the samples were marked on the ventral, caudal side with surgical thread to maintain orientation. These were then placed in labeled histology cassettes.

Histological processing was performed by Melika Muzaferovic-Majdanac under supervision of Dr. Teresa Pirker. The retrieved samples were fixed in 4% formalin for at least 24 hours and then transferred to PBS (phosphate-buffered saline) solution, where they were stored under cooling conditions. Next, the samples were dehydrated using an ascending alcohol series and xylene, followed by embedding in paraffin.

After sectioning with a microtome, the samples were deparaffinized using a descending alcohol series and rinsed with distilled water.

For HE-staining the samples were stained with hematoxylin for 10 minutes. Following rinsing with distilled water and bluing with an ammonia solution, the samples were stained with 1% eosin for 5 to 60 seconds. The samples were then dehydrated again using an ascending alcohol series, cleared with xylene, and permanently mounted with Cytoseal.

For Sirius Red staining, the samples were stained with Weigert's iron hematoxylin for 15 minutes. They were then rinsed with water and placed in distilled water for one hour. Following this, the samples were stained with Picrosirius Red for one hour, treated with acetic acid, dehydrated again using an ascending alcohol series, cleared with xylene, and permanently mounted with Cytoseal.

For Masson-Goldner-Trichrome staining, the samples were stained with Weigert's iron hematoxylin for 2 minutes. After rinsing with water, they were stained with Ponceau-Acid Fuchsin, Phosphotungstic Acid-Orange G, and Light Green SF, each for 5 minutes. After each staining step, the samples were rinsed with 1% acetic acid. The samples were then rinsed with distilled water, dehydrated using an ascending alcohol series, cleared with xylene, and permanently mounted with Cytoseal.

After staining, the samples were mounted on glass slides and fixed for microscopic examination. The Olympus BX43 microscopen (EVIDENT Europe GmbH, Hamburg, Germany) was used for the analysis. An overview image at 100x magnification and images of representative areas of the sample at 200x magnification were captured for each specimen.

Initially, overview images of the HE-stained samples were taken at 100x magnification. Since HE staining provides a broad overview and muscle fibers can be identified even at 100x magnification, images at 200x magnification were deemed unnecessary for these samples.

Subsequently, for the Sirius Red and Masson-Goldner-Trichrome stained sections, one overview image at 100x magnification was taken for each sample. Following this, three representative areas of the sample were selected, and images were captured at 200x magnification.

If the sample appeared highly heterogeneous (with several large areas of differing composition), one image was taken at 200x magnification in each of the distinct areas. If the sample appeared relatively homogeneous (a large area with a uniform appearance and only small parts of variation), images were taken within the large, homogeneous area.

The images taken at 200x magnification were analyzed using the FIJI ImageJ image processing software and the Color Deconvolution Tool (45,46). A macro was created for

each staining type so that all samples of a given staining were processed with identical settings.

The Sirius Red-stained samples were processed in such a way that the collagen fibers were color-coded according to their orientation within a range from -90° to +90°. This color coding allowed a visual representation of the fiber orientation. Additionally, FIJI generated datasets indicating the number of fibers in each orientation. These data were used for statistical analysis in SPSS.

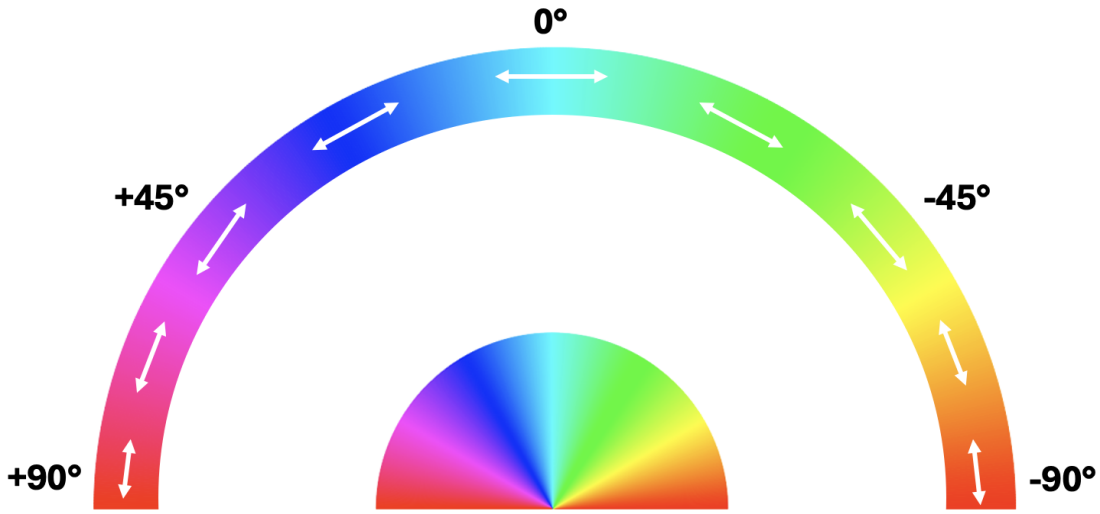

Figure 10: *Circular color coding according to fiber orientation.*
Vertical orientated fibers are displayed in red tones, horizontal fibers in blue tones.
Created by author.

The Masson-Goldner trichrome-stained samples were processed using FIJI ImageJ to differentiate the red-stained smooth muscle fibers from the differently colored tissues and to display them separately using a black-and-white image. This enabled assessment of the percentage of muscle tissue relative to the total tissue in each subregion. These data were also analyzed in SPSS.

3. Results

3.1. Macroscopy of embalmed pelves

The following description of the dissection uses defined anatomical terms for positional relationships and directions. The sacrum is described as dorsal, and the attachment of the uterosacral ligament (USL) to the sacrum as sacral. The cervix and uterus are described as ventral, and the attachment of the USL to the cervix and uterus as cervical.

3.1.1. Gross anatomy of undissected embalmed pelves

After opening the abdominal wall, the anatomy of the 10 female pelves could be examined. Without exerting tension on the surrounding structures, the rectouterine fold (Plica rectouterina) could be identified in all specimens. However, in pelves with a prominent rectum (n=4), this fold could not be visualized in its whole extend. When traction was applied to the uterus ventrally and the rectum was moved laterally towards the pelvic wall, the rectouterine fold was more prominent.

After further investigation, in 8 specimens, connective tissue fibers, nerve fibers, and small blood vessels aligned with the direction of the USL could be identified, as they were visible through the peritoneum.

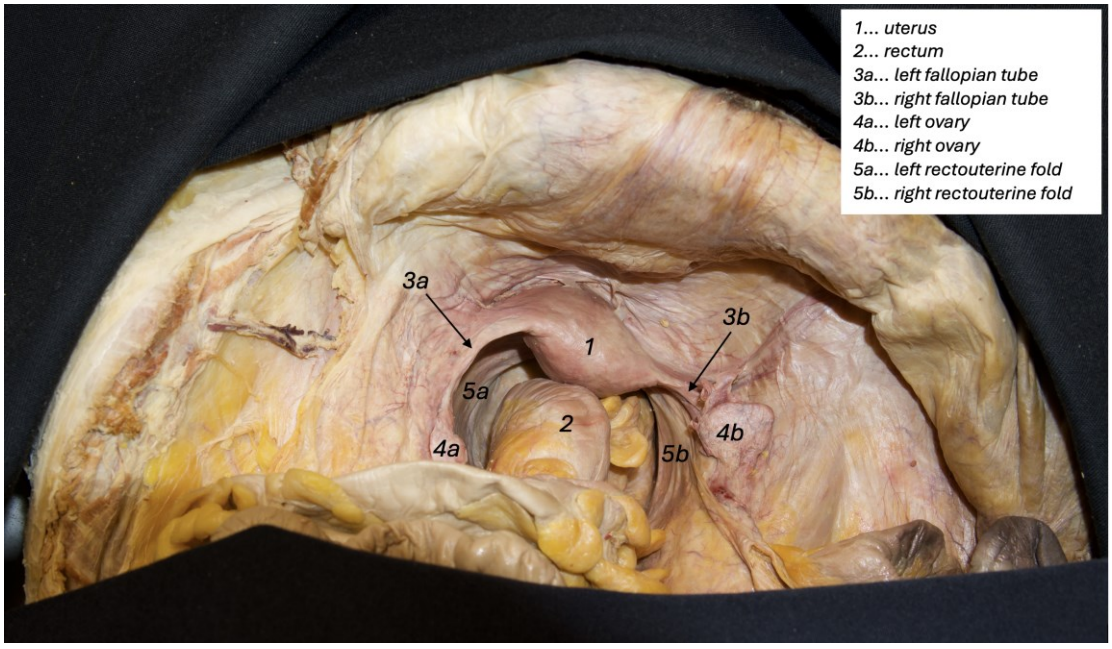

Figure 11: *Overview of undissected, fixated pelvis with intact pelvic organs and rectouterine fold.*

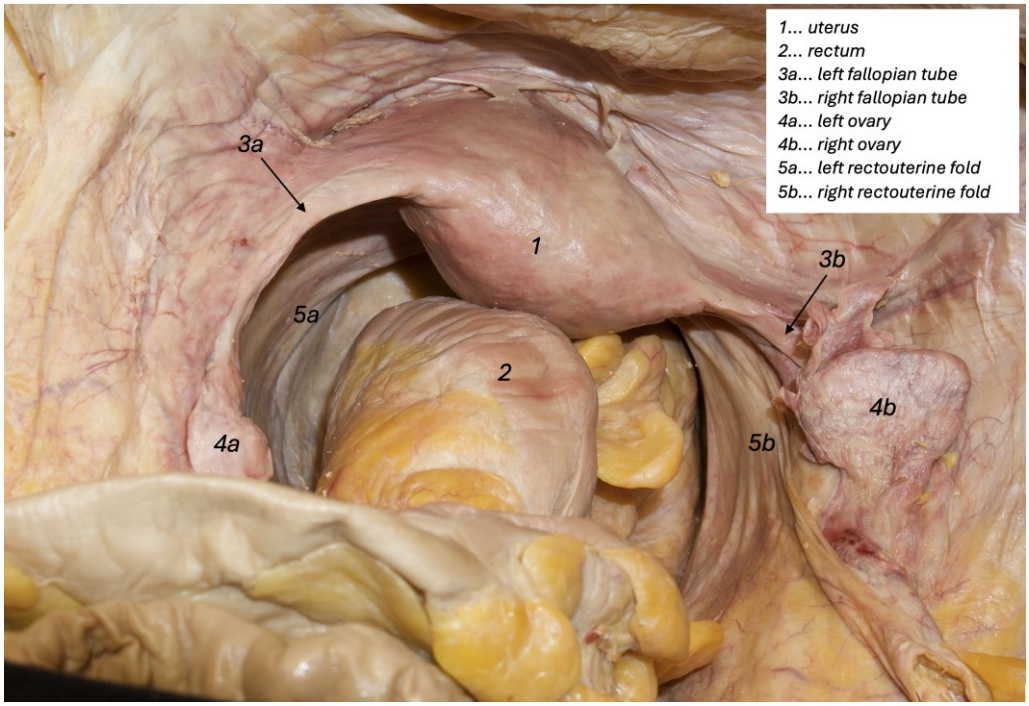

Figure 12:*Close up view of undissected, fixated pelvis.*
The pelvic organs are intact and the rectouterine folds (5a, 5b) are visible.

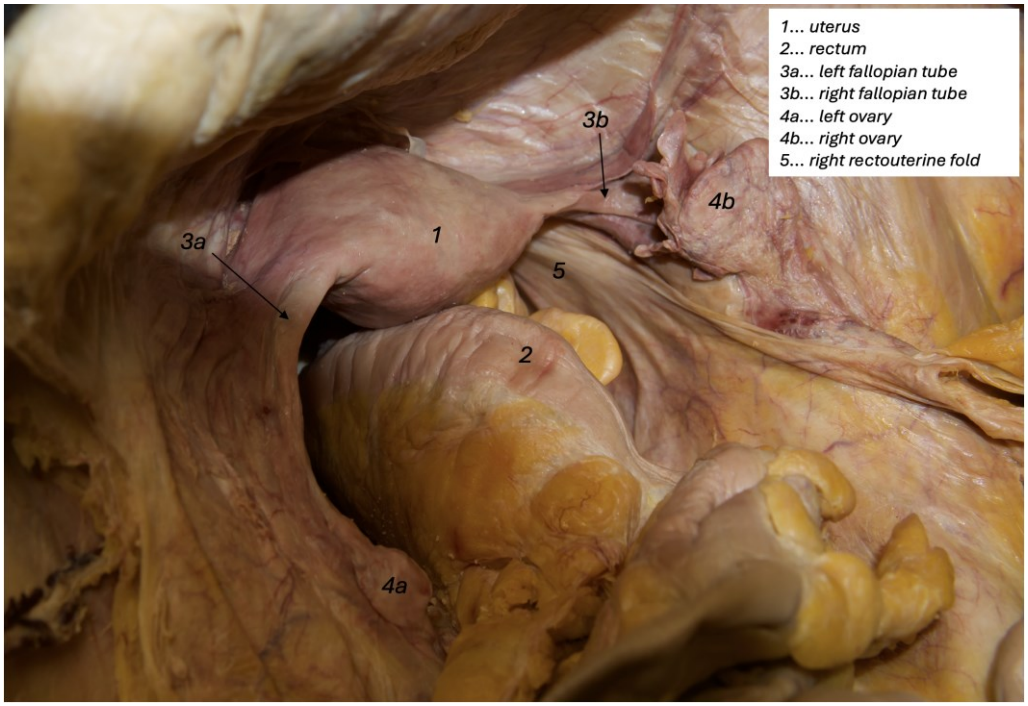

Figure 13: *View of undissected, fixated pelvis.*
The pelvic organs are intact and the right rectouterine fold (5) is clearly visible.

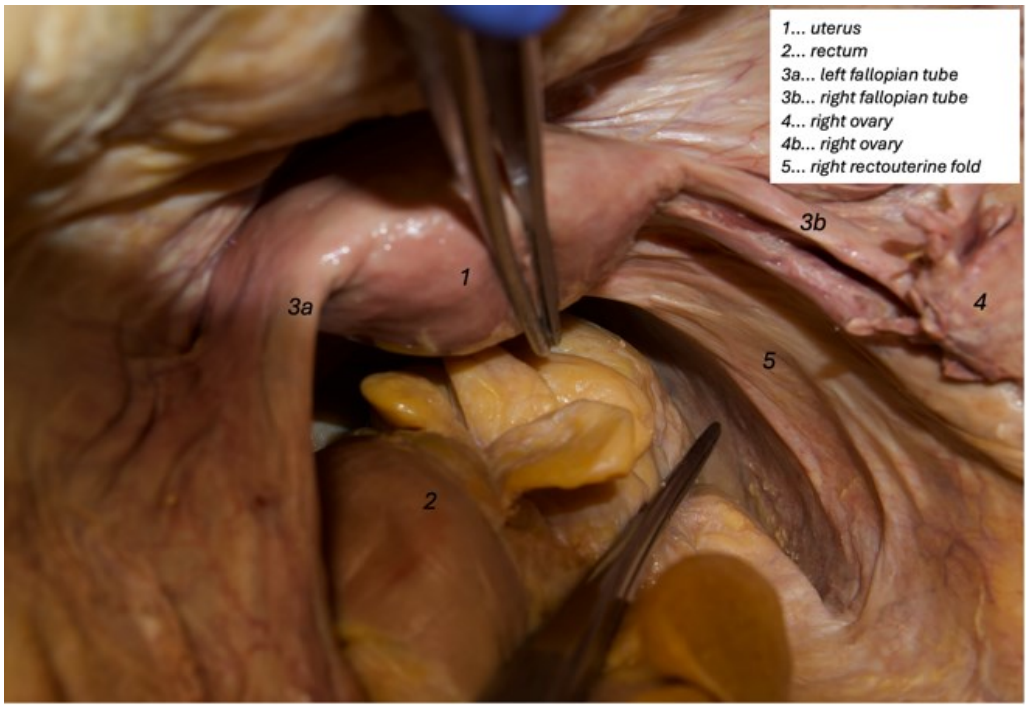

Figure 14: *Close up view of undissected fixated pelvis with ventral traction applied to the uterus. The right rectouterine fold is more prominent because of the traction applied.*

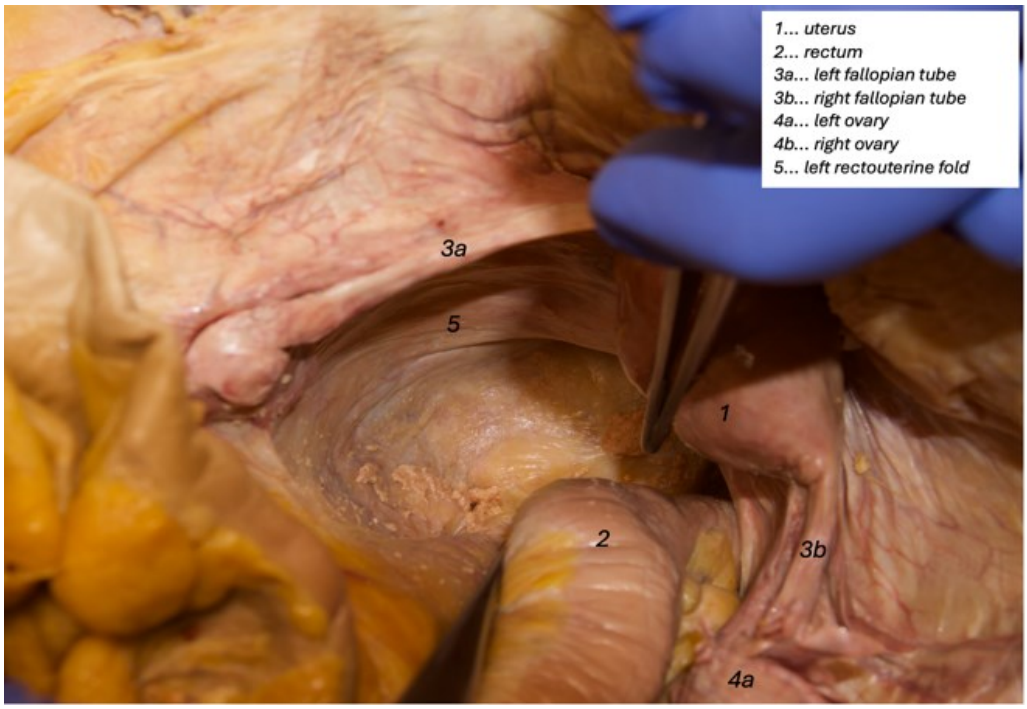

Figure 15: *Close up view of undissected fixated pelvis with ventral traction applied to the uterus. The left rectouterine fold is more prominent because of the traction applied.*

3.1.2. Measurements of undissected embalmed pelves

Before dissecting, the extend of the rectouterine fold was measured with a flexible ruler and notes were taken (ref. table 7).

When no traction was applied, the mean length (± standard deviation, SD) of the uterosacral ligaments in their ventro-dorsal extent was 9.7 (SD ± 1.87) cm (range 7.2 – 13.1 cm) on the left, and 11.8 (SD ± 1.92) cm (range 8.5 – 14.1 cm) on the right. These measurements were taken from the most dorsal point on the sacrum to the most ventral point on the cervix using a flexible ruler along the upper edge of the rectouterine fold.

When traction was applied to the uterus in a ventral direction, the extent was 10.4 (SD ± 1.61) cm (range 7.2 – 13.1 cm) on the left and 12.4 (SD ± 1.75) cm (range 9.2 – 15.0 cm) on the right.

Measurements of undissected embalmed pelves (n=3)				
Outer pelvic measurements	**Measurements in cm**			
Distantia interspinosa	**22.8 cm (SD ± 1.23 cm)**			
Distantia intercristalis	**26.0 cm (SD ± 1.76 cm)**			
Inner pelvic measurements				
Diameter transversa	**11.6 cm (SD ± 1.11 cm)**			
Conjugata anatomica	**11.5 (SD ± 0.95 cm)**			
Conjugata vera	**11.1 (SD ± 1.92 cm)**			
Uterosacral ligament				
Length curvilinear	Without traction		With traction applied to the uterus	
	Left	Right	Left	Right
	9.7 cm (SD ± 1.87 cm)	**11.8 cm (SD ± 1.92 cm)**	**10.4 cm (SD ± 1.61 cm)**	**12.4 cm (SD ± 1.75 cm)**
Distance between sacrum and cervix	**10.2 (SD ± 1.58)**			

Table 7: *Results - Measurements of undissected embalmed pelves.*

3.1.3. Gross Anatomy of dissected embalmed pelves

After dissection of the peritoneum, the connective tissue fiber bundles, blood vessels, and nerves could be examined more precisely. Most of the fibers were oriented in a ventro-dorsal direction, corresponding to the USL. These superficial layers were dorsally connected to the endopelvic fascia and to the peritoneum, ventrally to the cervix and the inferior part of the uterus.

However, fibers were also recognized that extended from the ventral or cervical area deeper into the direction of the pelvic arch. Attempts were made to trace these fibers, revealing that they are not arranged in a single plane but rather in different layers to form a three-dimensional network. The fibers of these deeper layers could be traced to the pelvic floor muscles. these fibers are not arranged in a single plane but rather form a three-dimensional network interconnected with the fascia of the pelvic floor muscles.

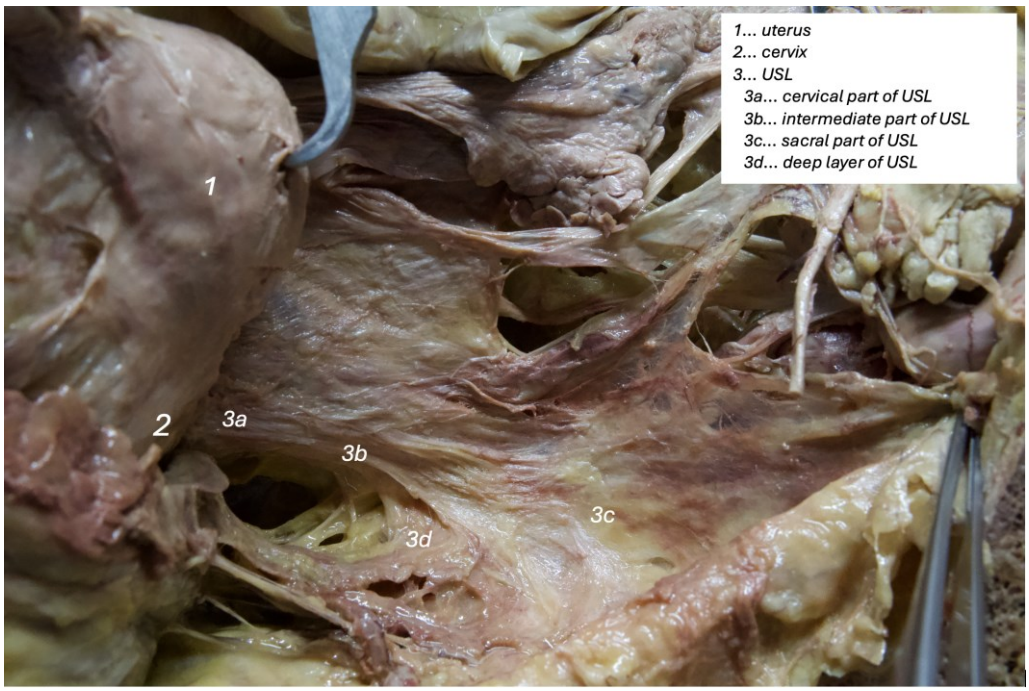

Figure 16: *Medial view of dissected, fixated right hemipelvis.*
After dissecting the peritoneum, fibers of the USL are clearly visible, especially in the cervical region.

In intact pelvises the insertion points at the uterus could be seen in most specimens. In those with a very prominent or ectatic rectum (n=4), the cervix could not be fully visualized.

Before resection of the peritoneum, the insertion points at the endopelvic fascia in the area of the second or first sacral segments could be visualized in all samples when traction was applied to the uterus in a ventral direction.

After dissecting the peritoneum, the insertion points, particularly at the cervix, could be displayed very clearly. The fibers were bundled into dense groups.

The visualization of the sacral insertion point was more difficult due to the anatomy of the USL. Unlike the insertion points at the uterus, it had a large craniocaudal extent and was very decreased in width. The rectouterine fold at the sacrum resembled more of a thin connective tissue sheet than a distinct ligament.

By applying tension, fibers could be tightened that connected with the endopelvic fascia. However, no firm connections to the sacral bone itself could be identified.

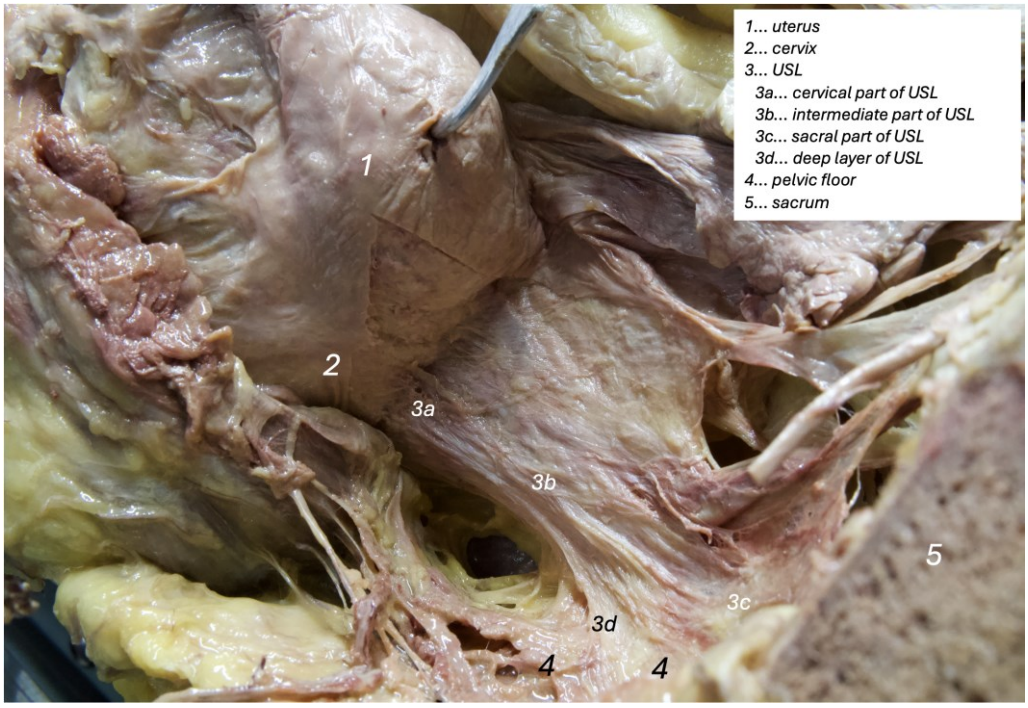

Figure 17: *Dissected right USL, medial view.*
Also visible: fibers of the deep layer of the USL connecting to the pelvic floor.

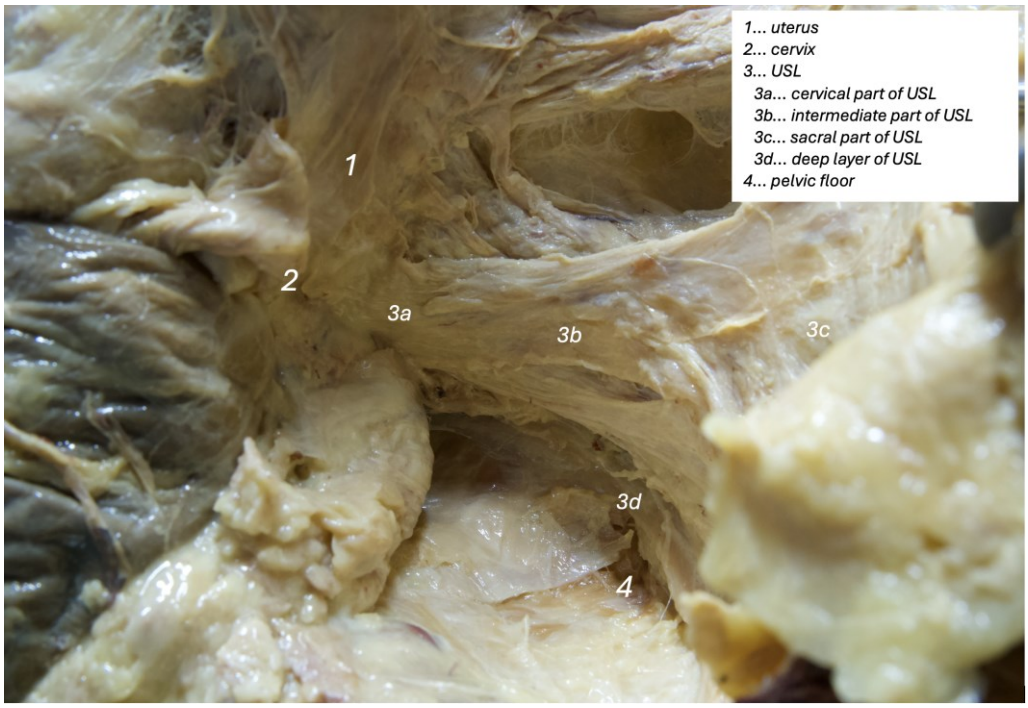

Figure 18: *Dissected right USL, medial view.*
Different specimen with also visible fibers of connective tissue in direction of the USL´s extend and visible pelvic floor muscles (4).

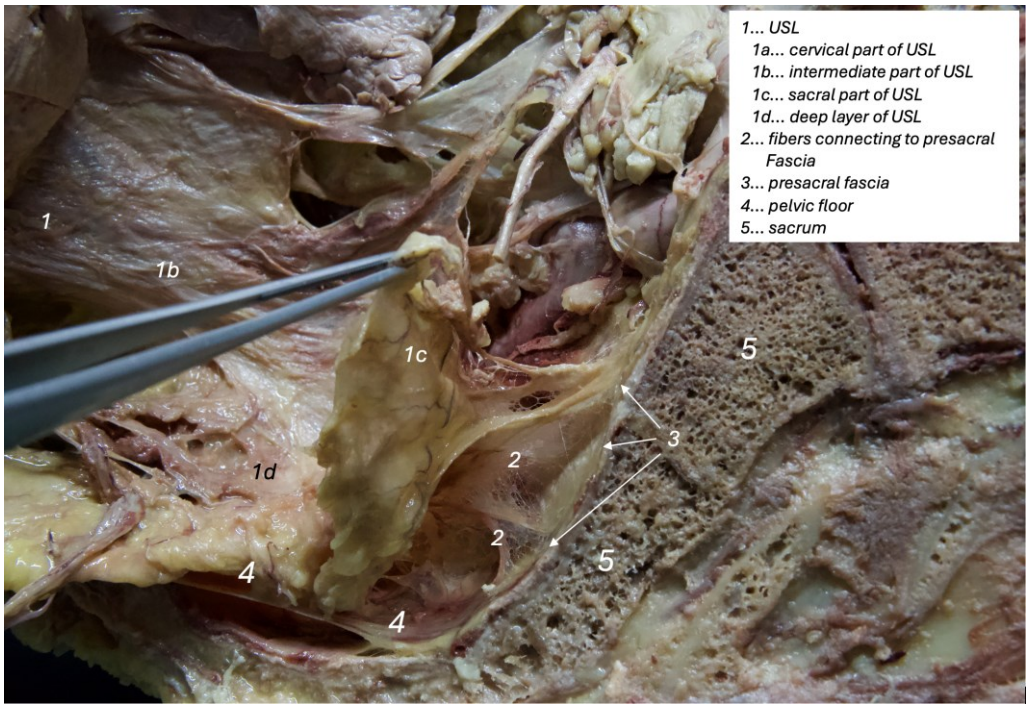

Figure 19: *Dissected right USL, medial view.*
When traction is applied to the sacral part of the USL, connective fibers are visible that link to the endopelvic fascia.

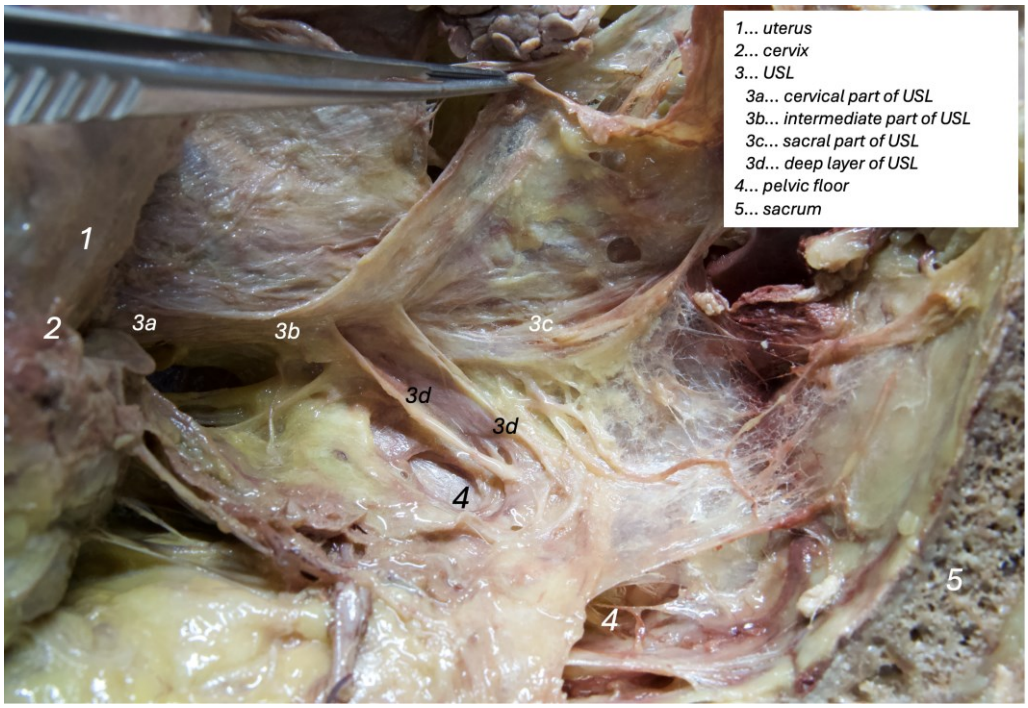

Figure 20: *Dissected right USL, medial view.*
Visualization of the different layers and the three-dimensional structure of the USL.

Aspects of macroscopic assessment (4 specimen, 4 left and 4 right USL, n=8)		
Connective tissue fibers		
Fibers visible	Yes	No
	8	**0**
Size of fibers	Large (>1 mm)	Small (<1mm)
	4	**4**
Nervous fibers		
Nervous fibers visible	Yes	No
	6	**2**
Insertion points		
Cervical insertion points visible	Yes	No
	8	**0**
Sacral insertion points visible	Yes	No
	8	**0**
Deep layer and insertion points at pelvic floor visible	Yes	No
	6	**2**

Table 8: *Results - Aspects of macroscopic assessment.*

3.1.4. Measurements of dissected embalmed pelves

After dissection and full exposure of the entire USL, the measurements were repeated in the same manner. It showed a mean ventro-dorsal extent of 11.8 (SD ± 1.16) cm (range 10.5 to 12.5 cm) without traction applied to the uterus.

Thickness and width of the USL was measured at the sacrum, the ischial spine and the cervix. The mean thickness at the sacrum was 0.2 (SD ± 0.06) cm, at the ischial spine 0.3 (SD ± 0.06) cm and at the cervix 0.4 (SD ± 0.17) cm. The mean width at the sacrum was 6.5 (SD ± 0.55) cm, at the ischial spine 4.3 (SD ± 0.76) cm and at the cervix 3.4 (SD ± 0.66) cm.

Measurements of dissected embalmed pelves		
Uterosacral ligament right	**Measurements in cm**	
Length curvilinear	**11.8 cm (SD ± 1.16)**	
Distance between sacrum and cervix	**8.8 cm (SD ± 1,.23)**	
Thickness	at sacrum	**0.2 cm (SD ± 0.06)**
	at ischial spine	**0.3 cm (SD ± 0.06)**
	at cervix	**0.4 cm (SD ± 0.17)**
Width	at sacrum	**6.5 cm (SD ± 0.55)**
	at ischial spine	**4.3 cm (SD ± 0.76)**
	at cervix	**3.4 cm (SD ± 0.66)**

Table 9: *Results - Measurements of dissected embalmed pelves.*

After taking in situ measurements, the dissected USL were extracted from the pelvis. The ligaments were then histologically processed and examined as described in the methods section (Section 2.3.)

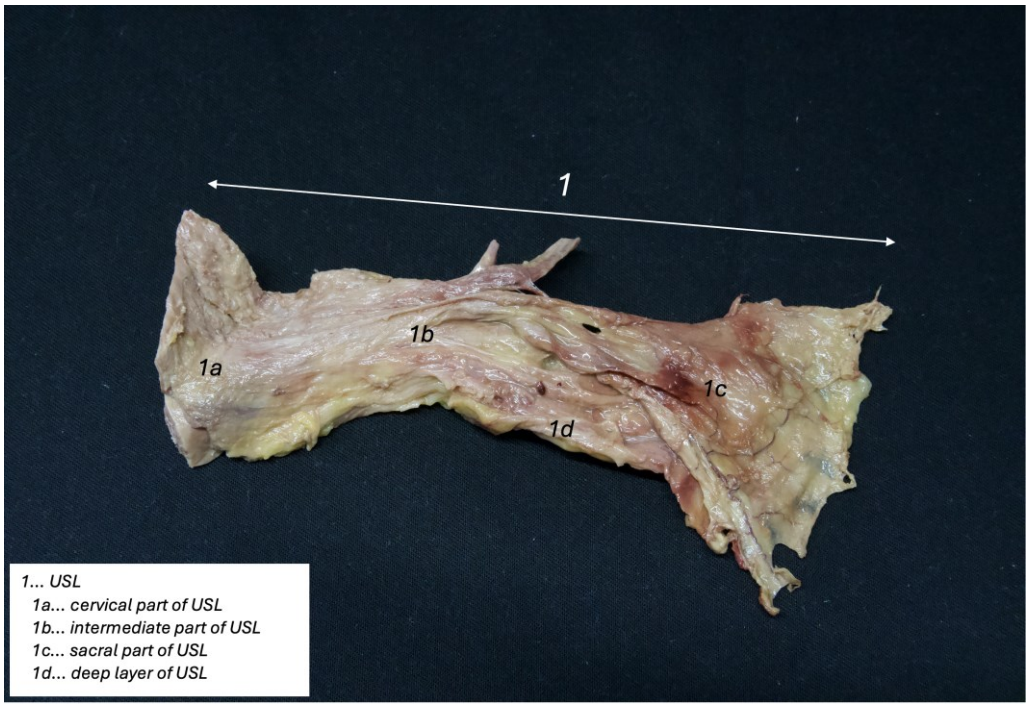

Figure 21: *Dissected and extracted USL 1.*

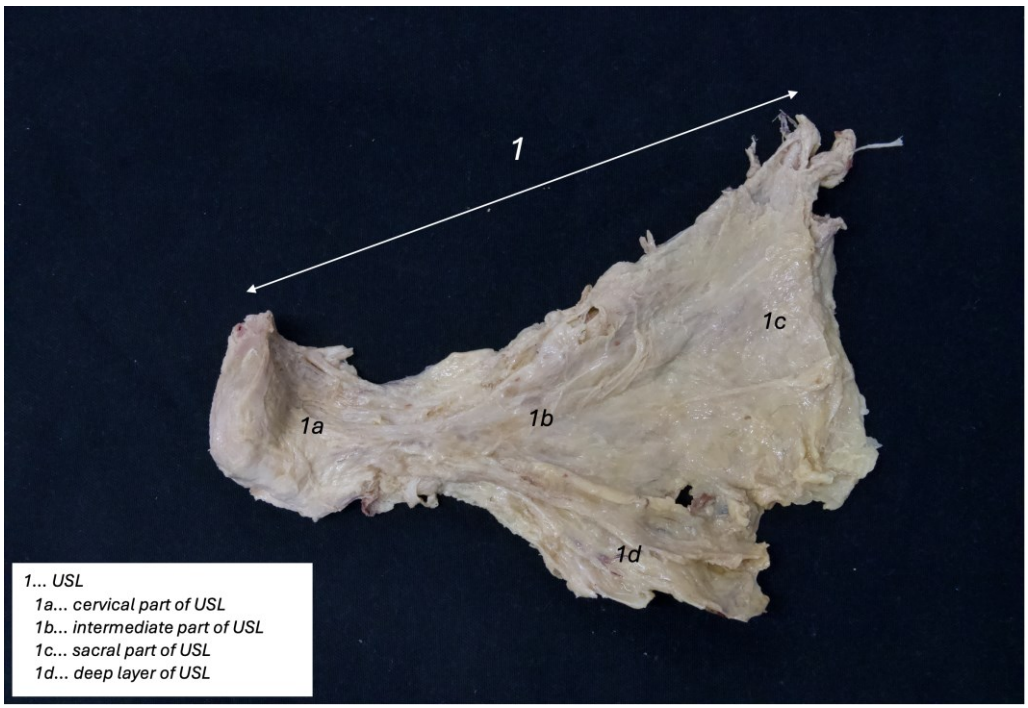

Figure 22*: Dissected and extracted USL 2.*

Figure 23: *Dissected and extracted USL 3.*

3.2. Macroscopy of unembalmed pelves

In contrast to the fixed specimens, which were well-suited for macroscopic examination due to the condition of the tissue, the unfixed specimens were primarily used for harvesting the USL for histological analysis.

3.2.1. Dissection of unembalmed pelves

As described in the methods section, a modified POP-Q score was applied to the unfixed body donors before opening the abdominal wall and dissecting the uterosacral ligaments (USL) to detect potential prolapse conditions post mortem. First, the distance from the cervix to the hymen was measured and documented without any manipulation. In a second step, a traction force of 500 g was applied to the cervix using a spring scale, and the distance from the cervix to the hymen was measured again.

The following distances were measured and documented:

Adapted POP-Q-Score for unembalmed specimen		
# of specimen	**Measurements cervix hymen without traction in cm**	**Measurements cervix hymen without traction in cm**
L66	**-5.5**	**-3.5**
L84	**-4**	**-2**
M47	**-6.5**	**-4**
M100	**-4.5**	**-2.5**
M104	**-6**	**-3**
M127	**-6.5**	**-2.5**
M128	**-5**	**-1.5**
N36	**-8**	**-3.5**
N40	**-7.5**	**-3**
N45	**-5.5**	**-3.5**
P26	**-6.5**	**-2.5**
L-1575-23	**-7**	**-6.5**
L1644-23	**-5.5**	**-2**

Table 10: *Measurements with adapted post-mortem POP-Q-Score.*

When comparing the measurements with Table 11, it becomes evident that all examined specimens showed at most a stage I prolapse, as the cervix remained at least 1 cm proximal to the hymen even under applied traction.

Stage	Characteristics
Stage 0	No prolapse; anterior and posterior points are all −3 cm, and C or D is between −TVL and −(TVL − 2) cm.
Stage I	The criteria for stage 0 are not met, and the most distal prolapse is more than 1 cm above the level of the hymen (less than −1 cm).
Stage II	The most distal prolapse is between 1 cm above and 1 cm below the hymen (at least 1 point is −1, 0, or +1).
Stage III	The most distal prolapse is more than 1 cm below the hymen but no further than 2 cm less than TVL.
Stage IV	Represents complete procidentia or vault eversion; the most distal prolapse protrudes to at least (TVL − 2) cm.

Table 11: *Stages of Pelvic Organ Prolapse, Boyles et al. (11).*

3.3. Histology of embalmed and unembalmed pelves

Histological analysis was initially performed separately for embalmed (n=3) and unembalmed (n=13) USL, as the samples were collected at different time points. However, since the embalmed tissue samples could also be processed and evaluated histologically to the same standard, the two groups were ultimately analyzed together (n=16).

At this point, the exact labeling of the individual samples should be reiterated:

- **Sample:** Tissue sample taken from the USL
- **Subregion:** Specific localization of the sample within the USL
    - Cervical
        - cervical superficial **(Csup)**
        - cervical deep **(Cprof)**
    - Intermediate
        - intermediate superficial **(Isup)**
        - intermediate deep **(Iprof)**

- Sacral
    - sacral superficial (**Ssup)**
    - sacral intermediate **(Sint)**
    - sacral deep **(Sprof)**

- **Region:** Grouping of subregions within one section of the USL
    - Csup + Cprof = **Cervical region**
    - Isup + Iprof = **Intermediate region**
    - Ssup + Sint + Sprof = **Sacral region**

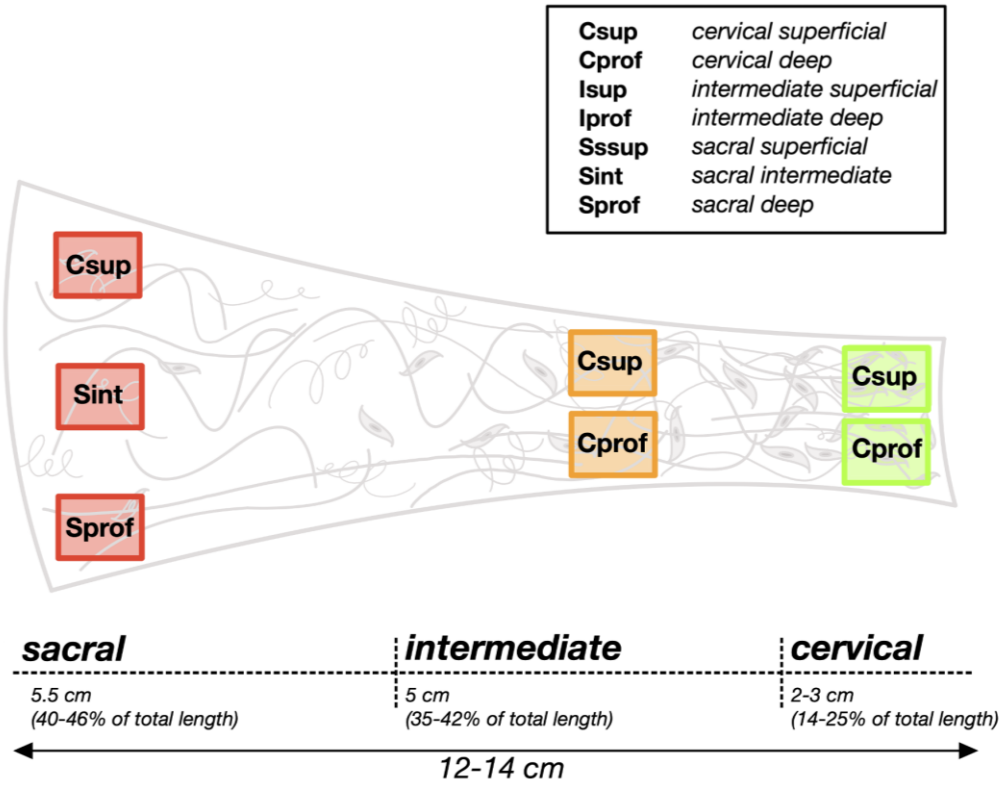

Figure 24: *Division of USL in cervical, intermediate and sacral section.*
To improve readability figure 9 is shown here again.
Created by author using Notability.

From each extracted USL (n=16), one sample was taken from each specified subregion and stained using the histological techniques described above (Chapter 2.5.). Subsequently, all samples of a specific subregion were examined microscopically. For each sample, three images were captured at 200x magnification.

3.3.1. Microscopical analysis

Initially, the acquired histological images were visually examined for their components and overall composition.

In HE-staining, the cervical part revealed bundles of smooth muscle tissue, both superficially and deeply. Smooth muscle was identified as the main component of the cervical region samples. In addition, connective tissue, small blood vessels, and small bundles of nerve fibers were observed between the muscle fibers.

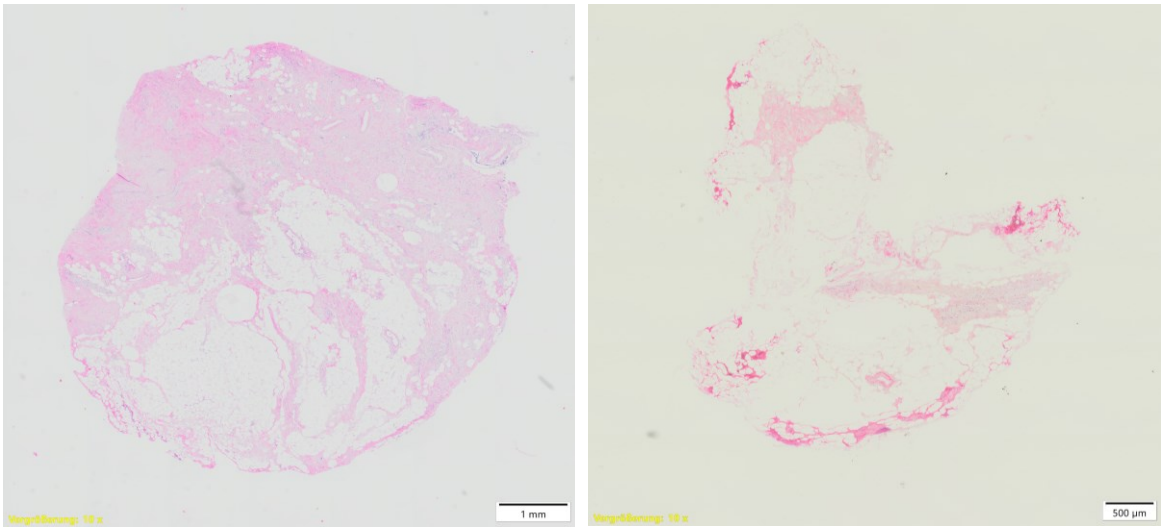

A: USL cervical deep HE staining *B: USL intermediate superficial HE staining*

Figure 25: *Examples of HE stained samples of the USL in 100x magnification*

A notable finding was the clear interindividual variation in tissue composition. For instance, in some USL samples (e.g. N36), a high proportion of muscle tissue was present in all samples from the cervical region, whereas in samples from another USL (e.g. L66), a lower muscle content was observed across the same region.

In the intermediate region, the amount of smooth muscle decreased compared to the cervical region. The prominent blood vessels typical of the cervical region were also progressively reduced. In contrast, the proportion of connective tissue increased, becoming the main component of the USL in this region. Again, interindividual differences in the composition of the various tissue components were observed.

The sacral part consisted almost entirely of loose connective tissue, interspersed with adipose tissue and very few muscle fibers.

3.3.2. Data acquisition

Collagen fiber orientation:

The acquired images were subsequently analyzed using the methods described above (chapter 2.5.) with FIJI ImageJ Software. Using Sirius Red staining, the collagen fibers were stained and then isolated in FIJI using the Color Deconvolution tool, allowing for independent assessment of the collagen content.

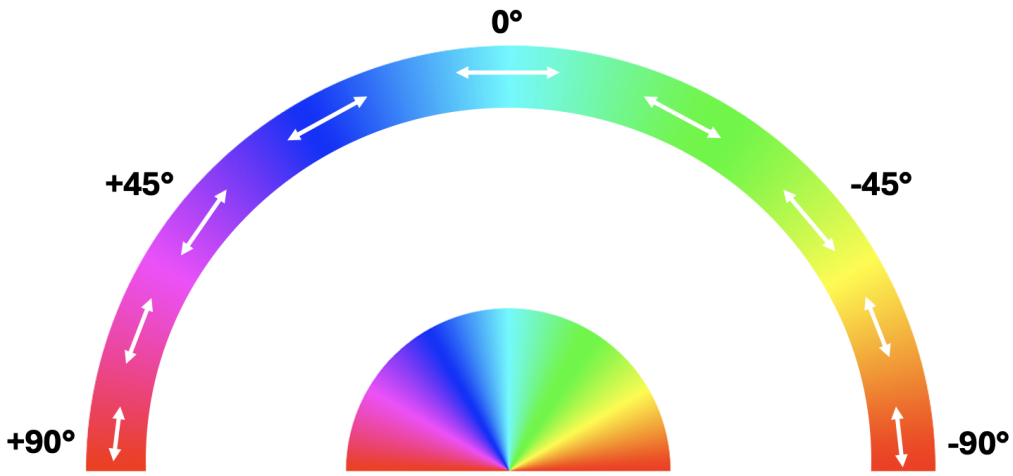

Figure 26: *Circular color coding according to fiber orientation.*
Vertical orientated fibers are displayed in red tones, horizontal fibers in blue tones.
Created by author.

Since the data were not normally distributed according to statistical analysis, the following results are reported as medians (Q2), including the 25% (Q1) and 75% (Q3) quartiles (ref. table 12).

The fibers in the superficial cervical subregion were oriented in a median -9.75° (Q1: -24.67°; Q3: 6.88°) angle. In the deep cervical subregion, the fibers were oriented in a median 3.77° (Q1: -23.38°; Q3: 22.13°) angle.

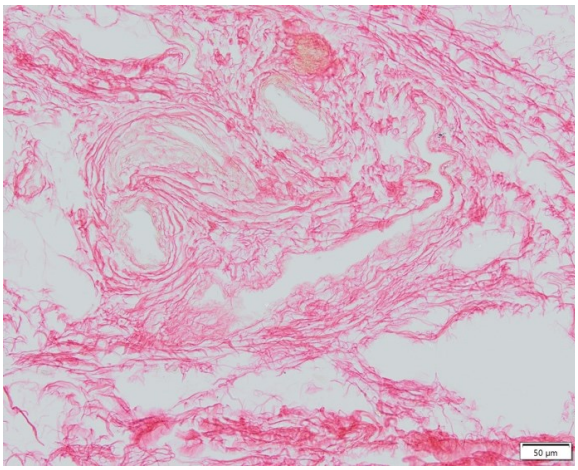

A: USL cervical superficial Sirius red original.

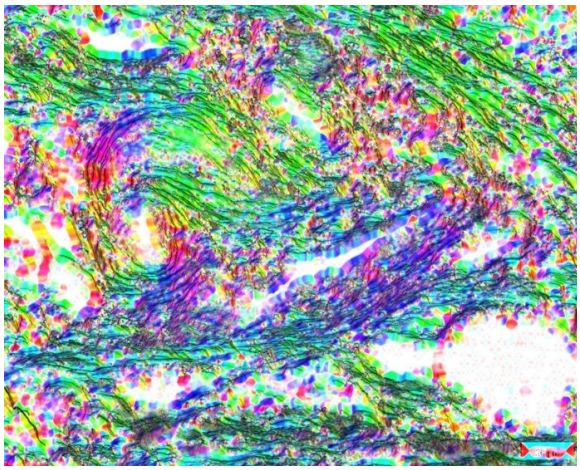

B: USL cervical superficial color coded according to fiber orientation.

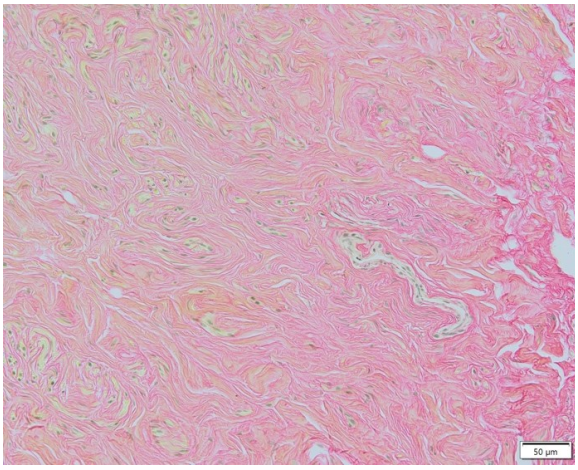

C: USL cervical deep Sirius red original.

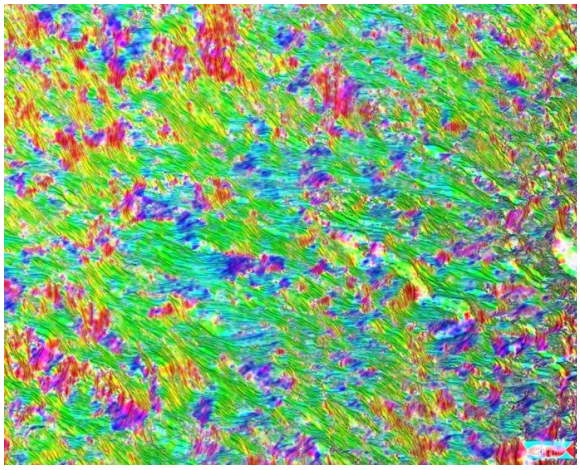

D: USL cervical deep color coded according to fiber orientation.

Figure 27: *Cervical part of the USL in Sirius red staining. A+B: superficial part, C+D: deep part.*

In the intermediate region, the collagen fibers in the superficial subregion were oriented in a median 19.01° (Q1: -7.74°; Q3: 61.56°) angle, while the fibers in the deep subregion had an orientation in a median 11.19° (Q1: -16.11°; Q3: 20.97°) angle.

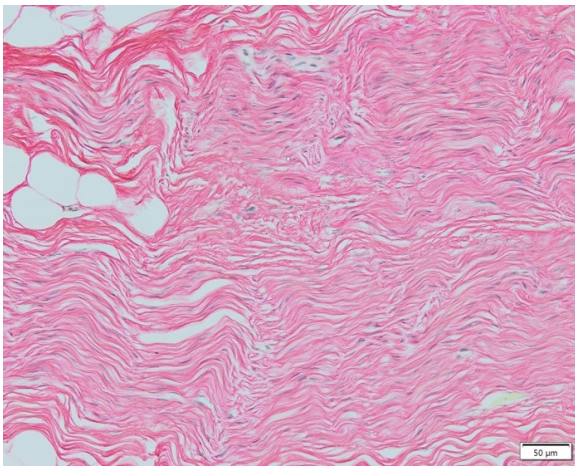

A: USL intermediate superficial Sirius red original.

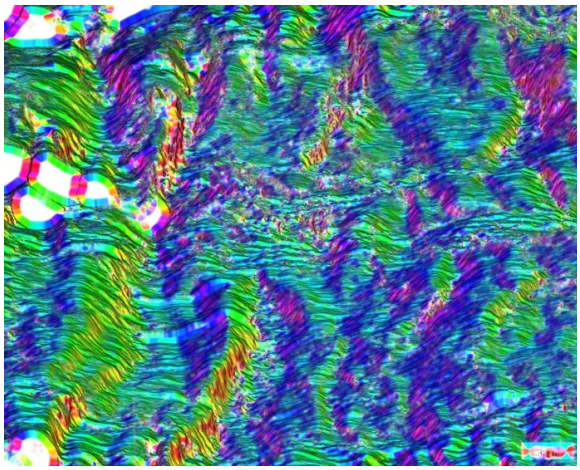

B: USL intermediate superficial color coded according to fiber orientation.

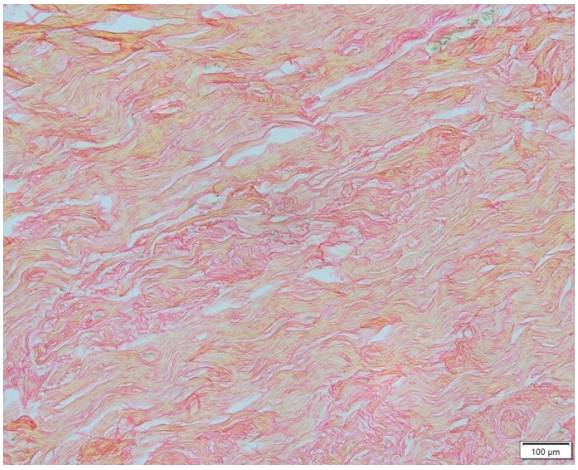

C: USL intermediate deep Sirius red original.

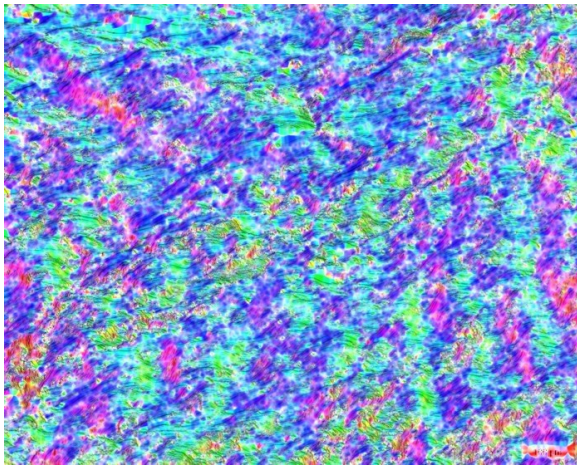

D: USL intermediate deep color coded according to fiber orientation.

***Figure 28**: Intermediate part of the USL in Sirius red staining.*
A+B: superficial part, C+D: deep part.

In the sacral region the collagen fibers that could be identified showed a median orientation in a -21.06° (Q1: -32.67°; Q3: 8.90°) angle in the superficial, a median 2.68° (Q1: -17.70°; Q3: 34.92°) angle in the intermediate and a median 4.66° (Q1: -32.21°; Q3: 16.51°) angle in the deep subregion.

The orientation of the collagen fibers differs significantly between the young group and the aged group, particularly in the subregions Csup and Isup. However, due to the low number of samples, no statistical conclusions could be drawn (ref. table 12).

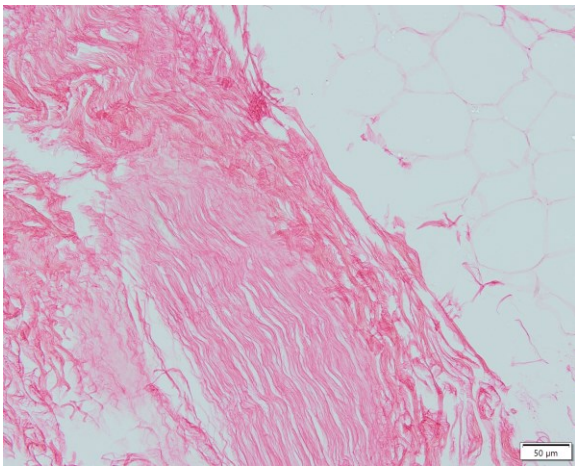

A: USL sacral superficial Sirius red original.

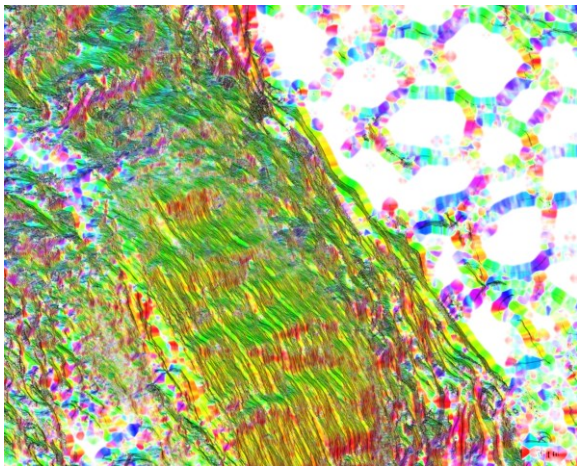

B: USL sacral superficial color coded according to fiber orientation.

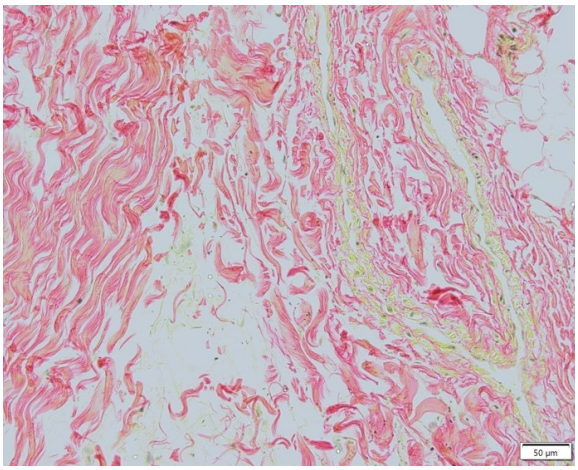

C: USL sacral intermediate Sirius red original.

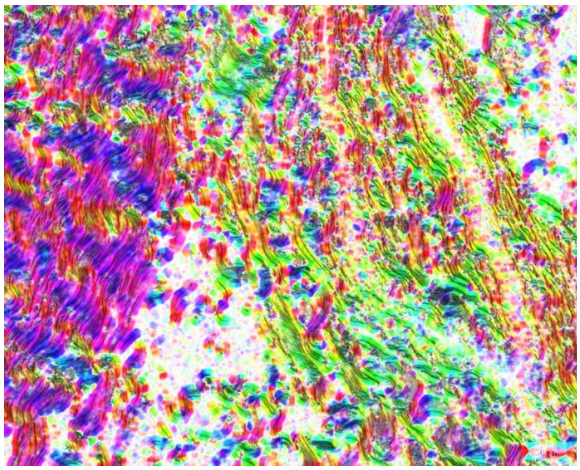

D: USL sacral intermediate color coded according to fiber orientation.

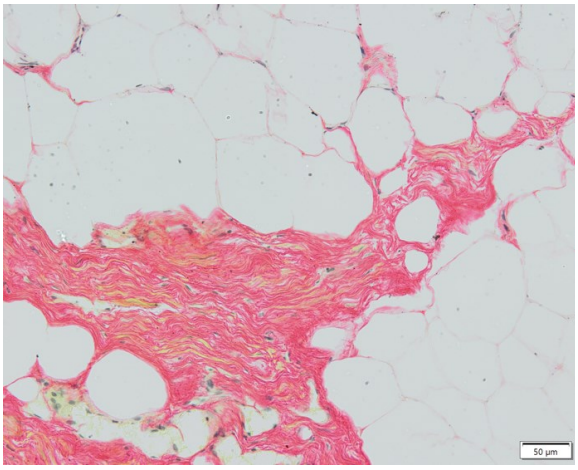

E: USL sacral deep Sirius red original.

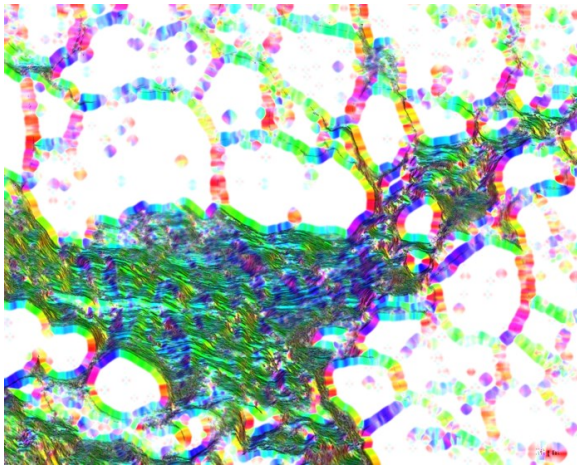

F: USL sacral deep color coded according to fiber orientation.

Figure 29: *Sacral part of the USL in Sirius red staining.*
A+B: superficial part, C+D: intermediate part, E+F: deep part.

Collagen Fiber Orientation			
Region	**Orientation in ° WHOLE**	**Orientation in ° AGED**	**Orientation in ° YOUNG**
Csup	**-9.75** Q1: -24.67 Q3: 6.88	**-8.36** Q1: -21.98 Q3: 8.43	**-47.149** Q1: -54.97 Q3: -29.14
Cprof	**3.77** Q1: -23.38 Q3: 22.13	**4.24** Q1: -23.00 Q3: 41.42	**0.81** Q1: -43.87 Q3: 3.33
Isup	**19.01** Q1: -7.74 Q3: 61.56	**13.68** Q1: -6.94 Q3: 56.23	**58.77** Q1: 9.25 Q3: 69.35
Iprof	**11.19** Q1: -16.11 Q3: 20.97	**8.49** Q1: -9.83 Q3: 20.96	**14.28** Q1: -34.80 Q3: 18.19
Ssup	**-21.06** Q1: -32.67 Q3: 8.90	#	##
Sint	**2.68** Q1: -17.70 Q3: 34.92	#	##
Sprof	**4.66** Q1: -32.21 Q3: 16.51	#	##
# Values for the aged cohort are the same as those for the whole cohort, as there are no samples in the young cohort *## No samples in the young cohort*			

Table 12: *Collagen fiber orientation.*

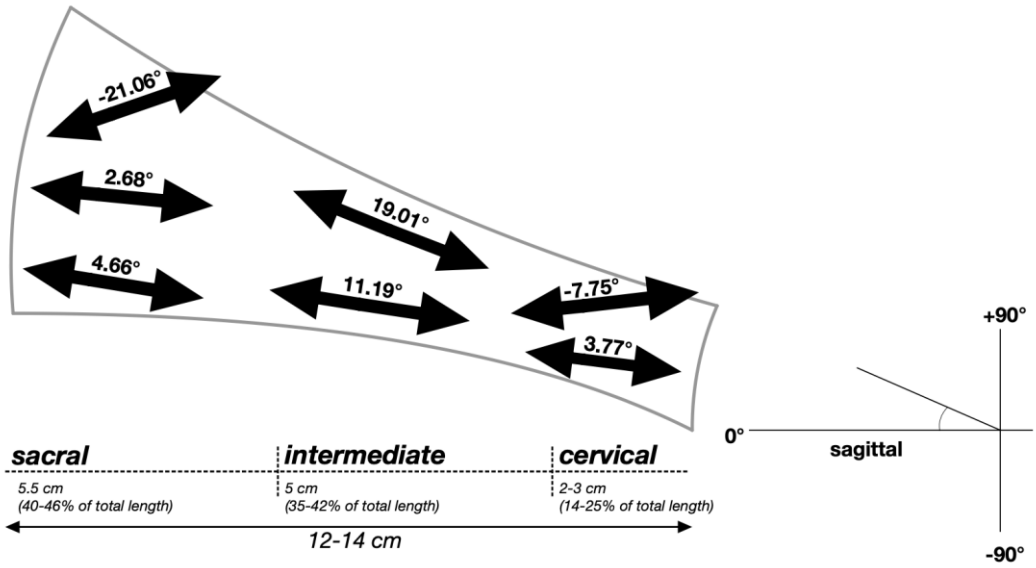

Figure 30: *Collagen fiber orientation in different subregions of the right USL (lateral view).*
For histological analysis the caudal ventral corner of each sample was marked. Therefore, all angles were calculated in respect to the sagittal axis.
Created by author using Notability.

Smooth muscle content:

Using Masson-Goldner-Trichrome staining and FIJI software the analysis of the cervical region showed a percentual amount of smooth muscle in the whole cohort (n=16) of 18.00 % (Q1: 10.22%; Q3: 44.45%) in the superficial subregion and 14.22% (Q1: 5.82%; Q3: 31.53%) in the deep subregion, compared to the overall amount of tissue.

The percentage of smooth muscle fibers in the cervical region relative to the total tissue is noticeably higher in the examined young group (n=2) compared to the aged group (n=14). However, due to the small sample size and the absence of samples from the sacral region from the young group, statistical significance cannot be demonstrated.

The percentual amount of smooth muscle in the intermediate region was 11.54% (Q1: 4.55%; Q3: 46.05%) in the superficial and 24.69% (Q1: 6.68%; Q3: 43.77%) in the deep subregion, compared to the total amount of tissue.

The percentual amount of smooth muscle in the sacral region was 15.11% (Q1: 2.42%; Q3: 39.13%) in the superficial, 16.95% (Q1: 6.69%; Q3: 37.38%) in the intermediate and 8.45% (Q1: 1.32%; Q3: 24.16%) in the deep part, compared to the total amount of tissue (ref. table 13).

Muscle content			
Region	%Muscle/Tissue WHOLE	%Muscle/Tissue AGED	%Muscle/Tissue YOUNG
Csup	18.00 Q1: 10.22 Q3: 44.45	17.92 Q1: 9.26 Q3: 17.92	42.31 Q1: 27.65 Q3: 65.82
Cprof	14.22 Q1: 5.82 Q3: 31.53	11.64 Q1: 5.02 Q3: 19.98	61.75 Q1: 41.69 Q3: 82.18
Isup	11.54 Q1: 4.55 Q3: 46.05	12.52 Q1: 3.72 Q3: 45.02	5.08 Q1: 3.26 Q3: 5.13
Iprof	24.69 Q1: 6.68 Q3: 43.77	#	##
Ssup	15.11 Q1: 2.42 Q3: 39.13	#	##
Sint	16.95 Q1: 6.69 Q3: 37.38	#	##
Sprof	8.45 Q1: 1.32 Q3: 24.16	#	##
# Values the aged cohort are the same as those for the whole cohort, as there are no samples in the young cohort *## No samples in the young cohort*			

Table 13: *Smooth muscle content.*

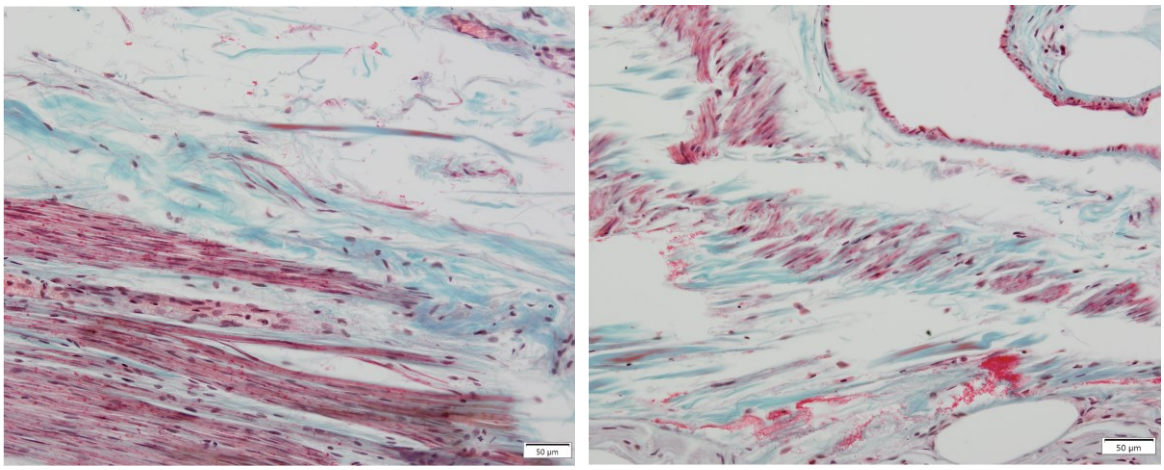

A: USL cervical superficial Masson-Goldner-Trichrome *B: USL cervical deep Masson-Goldner-Trichrome*

Figure 31: *Examples of Masson-Goldner-Trichrome stained samples of the USL in 200x magnification*

3.3.3. Statistical evaluation

From the FIJI-generated data of the three images per sample, the mean value was calculated. These values were then used for statistical analysis in SPSS Statistics (SPSS Version 29, IBM Corp.)

Collagen fiber orientation:

First, all seven subregions were analyzed (regardless of age) in relation to the orientation of collagen fibers. The Shapiro-Wilk test of normality and graphical evaluation using Q-Q plots indicated that the distribution of collagen fibers ($p > 0.05$) did not follow a normal distribution.

The boxplot diagram illustrates the orientation of collagen fibers across the seven distinct subregions of the USL, categorized as mentioned above. Clear differences in median values are evident: the intermediate region, particularly Isup, shows a markedly more positive fiber orientation, whereas Csup and Ssup tend to exhibit lower or even negative orientations. The degree of variability also differs regionally, with greater dispersion observed in ISup and Sint, and more consistent fiber alignment in Csup, Iprof, Ssup and Sprof.

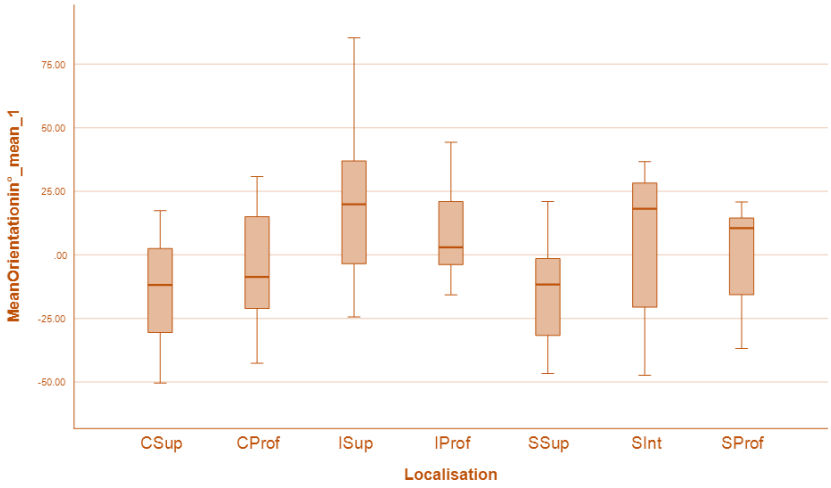

Figure 32: *Boxplot collagen fiber orientation.*

Using the Independent-Samples Kruskal-Wallis-Test, it was found that there was a statistically significant difference (p=0.043) between individual subregions in terms of fiber orientation. A following analysis using pairwise comparison (ref. table 14) showed a statistically significant difference in fiber orientation between the subregions Csup and Isup (p=0.024), and between Isup and Ssup (p=0.04).

Pairwise Comparisons of Orientation between Subregions					
Sample 1-Sample 2	Test Statistic	Std. Error	Std. Test Statistic	Sig.	Adj. Sig.[a]
Comparison of subregions of one region					
Csup - Cprof	-13.500	9.880	-1.366	0.172	0.688
Isup - Iprof	9.733	9.012	1.080	0.280	1.000
Ssup - Sint	-17.882	10.784	-1.658	0.097	0.776
Sint - Sprof	9.589	11.340	.846	0.398	1.000
Comparison between two adjacent subregions					
Csup - Isup	-27.533	9.352	-2.944	.003	0.024
Cprof - Iprof	-4.300	9.559	-.450	.653	1.000
Isup - Ssup	27.215	9.797	2.778	.005	0.04
Iprof - SProf	9.189	10.406	.883	.377	1.000

Each row tests the null hypothesis that the Sample 1 and Sample 2 distributions are the same.
Asymptotic significances (2-sided tests) are displayed. The significance level is .050.

Significance values have been adjusted by the Bonferroni correction for multiple tests.

Table 14: *Pairwise comparison between subregions: collagen fiber orientation.*

Based on the finding that there were no statistically significant differences concerning collagen fiber orientation within the subregions of the different regions, these subregions within a region were grouped (cervical, intermediate, sacral) and compared statistically (ref. table 15).

With respect to fiber orientation, statistically significant differences were found between the cervical and intermediate regions (p=0.008), and between the intermediate and sacral regions (p=0.015).

Pairwise Comparisons of Orientation between Regions					
Sample 1-Sample 2	Test Statistic	Std. Error	Std. Test Statistic	Sig.	Adj. Sig.[a]
Cervical - Intermediate	-13.562	4.541	-2.986	0.003	0.008
Intermediate - Sacral	13.771	4.905	2.807	0.005	0.015
Sacral - Cervical	.208	4.905	.042	0.966	1.000

Each row tests the null hypothesis that the Sample 1 and Sample 2 distributions are the same. Asymptotic significances (2-sided tests) are displayed. The significance level is .050.

Significance values have been adjusted by the Bonferroni correction for multiple tests.

Table 15: *Pairwise comparisons between regions: collagen fiber orientation.*

Smooth muscle content:

All seven subregions were analyzed (regardless of age) in relation to the content of smooth muscle. The Shapiro-Wilk test of normality and graphical evaluation using Q-Q plots indicated that the content of smooth muscle ($p > 0.05$) did not follow a normal distribution.

According to the smooth muscle content there was no statistically significant difference ($p > 0.05$) found between the different subregions. There was also no statistically significant difference ($p > 0.05$) within a region regarding smooth muscle content.

The boxplot illustrates the relative content of smooth muscle across the different subregions of the USL. Overall, there is considerable variability in all regions, particularly in Cprof, Isup, Ssup and Sint, where the range of values is especially wide. Median values differ between subregions: the highest median smooth muscle content is observed in the SSup region, whereas Cprof, Isup, and Sprof show comparatively lower median values. Despite subjectively noticeable differences in medians and variability, no clear regional trend, such as a continuous increase or decrease in muscle content along the ligament, can be identified and statistical analysis revealed no difference between subregions.

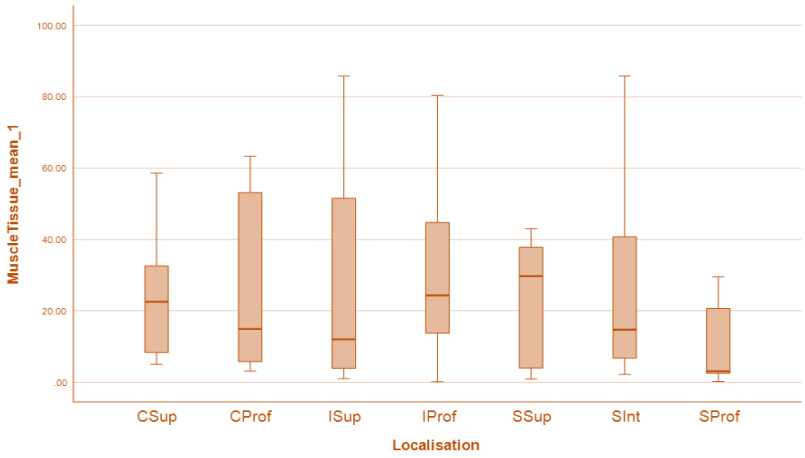

Figure 33: *Boxplot smooth muscle content.*

Using the Independent-Samples Kruskal-Wallis-Test, it was found that there was no statistically significant difference (p=0.745) between individual locations in terms of smooth muscle content. A following analysis using pairwise comparison also showed no statistically significant difference (p > 0.05) (ref. table 16).

Pairwise Comparisons of Muscle Content between Subregions					
Sample 1-Sample 2	Test Statistic	Std. Error	Std. Test Statistic	Sig.	Adj. Sig.[a]
Comparison of subregions of one region					
Csup - Cprof	3.750	9.142	0.410	0.682	1.000
Isup - Iprof	-5.786	9.142	-0.633	0.527	1.000
Ssup - Sint	-3.955	10.445	-0.379	0.705	1.000
Sint - Sprof	13.330	10.798	1.234	0.217	1.000
Comparison between two adjacent subregions					
Csup - Isup	8.036	8.783	.915	0.360	1.000
Cprof - Iprof	-1.500	9.487	-.158	0.874	1.000
Isup - Ssup	-.036	9.928	-.004	0.997	1.000
Iprof - Sprof	15.125	10.607	1.426	0.154	1.000

Each row tests the null hypothesis that the Sample 1 and Sample 2 distributions are the same.
Asymptotic significances (2-sided tests) are displayed. The significance level is .050.

Significance values have been adjusted by the Bonferroni correction for multiple tests.

Table 16: *Pairwise comparisons between subregions: smooth muscle content.*

Based on the finding that there were no statistically significant differences within regions, according to smooth muscle content, the subregions (superficial, intermediate, deep) within a region were pooled, and the regions (cervical, intermediate, sacral) and compared statistically (ref. table 17).

Pairwise Comparisons of Smooth Muscle between Regions					
Sample 1-Sample 2	Test Statistic	Std. Error	Std. Test Statistic	Sig.	Adj. Sig.[a]
Cervical - Intermediate	3.133	4.480	0.699	0.484	1.000
Intermediate - Sacral	0.067	4.751	0.014	0.989	1.000
Sacral - Cervical	3.200	4.751	0.673	0.501	1.000

Each row tests the null hypothesis that the Sample 1 and Sample 2 distributions are the same.
Asymptotic significances (2-sided tests) are displayed. The significance level is .050.

Significance values have been adjusted by the Bonferroni correction for multiple tests.

Table 17: *Pairwise comparisons between regions: smooth muscle content.*

With respect to smooth muscle content, no statistically significant differences were found between regions ($p > 0.05$).

Statistical analysis for both collagen fiber orientation and smooth muscle content was repeated within the "aged" group. The results were similar to those observed in the analysis of the total cohort.

Due to an insufficient number of samples, no analysis could be performed for the "young" group, but in general muscle content was considerably higher in the young group compared to the aged with up to a five times higher muscle content in specific regions (ref. table 14).

4. Discussion and Conclusion

The uterosacral ligaments play a significant role in pelvic organ support and stabilization and, along with the vesicovaginal ligament, it serves as the primary anchoring structure for the uterus and vagina in ventro-dorsal direction. This study examined the anatomical and histological characteristics of the USL and its microstructural differences in various regions in young and aged women. The aim was to derive potential functional implications and provide recommendations for possible surgical therapies in the treatment of pelvic organ prolapse.

4.1. Key findings

Our findings revealed a macroscopically observable regional heterogeneity of the USL with great interindividual differences and likely age differences. Macroscopically it was shown that the USL is particularly well-developed in the cervical region. In the middle and sacral regions, we observed that the USL becomes progressively thinner and fans out. Additionally, connections between the USL and the fascia of the pelvic floor muscles were documented. Thus, our study demonstrated that the USL is not merely a simple connection between the uterus, cervix, and sacrum but rather a complex three-dimensional structure.

Furthermore, interindividual differences in the dimensions of the USL were identified, particularly in the comparison between the left and right sides. We primarily attribute this to the asymmetrical left-sided position of the rectum in the pelvis. Our results indicate a greater lateral asymmetry of the USL than previously assumed (31), raising new questions regarding the functional significance of this variability.

Microscopic examination and the use of multiple staining techniques (including Hematoxylin-Eosin, Sirius Red, and Masson-Goldner-Trichrome) enabled a detailed examination and revealed distinct compositional differences across regions of the USL. Sirius Red staining highlighted the orientation of collagen fibers, which are essential for tensile strength and elasticity. Masson-Goldner-Trichrome staining revealed the spatial distribution of muscle fibers and connective tissue, providing additional evidence of regional variation within the ligament.

The histological analysis demonstrated that the cervical region was characterized by a high proportion of smooth muscle bundles, interspersed with connective tissue, small blood

vessels, and nerve fibers. In the intermediate region, the amount of smooth muscle decreased, while connective tissue became the predominant component. The sacral region was composed primarily of loose connective tissue and adipose tissue, with minimal smooth muscle content. However, clear interindividual variability in tissue composition was observed, particularly in the proportion of muscle fibers within corresponding regions of different USLs.

Quantitative analysis of collagen fiber orientation was performed using Sirius Red staining and FIJI software. Similarly, the relative smooth muscle content was quantified from Masson-Goldner-Trichrome-stained images.

Statistical analysis using SPSS included comparisons across both individual subregions and grouped regions (cervical, intermediate, sacral):

- Statistically significant differences in collagen fiber orientation were observed between Csup and Isup ($p=0.024$) and Isup and Ssup ($p=0.04$) and between the grouped cervical and intermediate region ($p=0.008$) and intermediate and sacral region ($p=0.015$).
- There was no statistically significant difference in smooth muscle content between subregions or within regions for the aged samples. The two young samples showed a much higher muscle content in the cervical region compared to the aged group.

These results indicate that the orientation of collagen fibers shows a region-specific organization, suggesting functional specialization along the ligament's length. One notable observation is the orientation of the collagen fibers in the subregion Ssup, which are not aligned in the expected direction. We suspect a connection with the difficulty of preparation in this area due to the delicate structure of this region. The distribution of smooth muscle remains relatively consistent within regions of the USL, although it was observed that the young group showed a noticeably higher muscle content (particularly in the cervical region) compared to the aged group. However, due to the small sample size in the young group ($n=2$), no statistical significance could be established in comparison to the aged group.

4.2. Comparison with previous studies

1.) The results of the macroscopic assessment are consistent with previous studies that have described the USL as a complex structure (9,31).The description of a well-

developed and clearly visible cervical region of the USL aligns with the findings of studies by Campbell et al.(23), Ramanah et al. (31) and Iwanaga et al. (26). Additionally, the fibers described in the study by Campbell et al. (23), Buller et al. (25) and Umek et al. (28), that extend caudally into the pelvic floor musculature were documented in 6 out of 8 dissected specimen. However, we also observed that, in the caudal region, these fibers are not arranged in a single plane but rather form a three-dimensional network interconnected with the fascia of the pelvic floor muscles.

2.) In contrast to the descriptions by Ramanah et al. our findings align with the studies by Campbell et al. (23), and Buller et al. (25), that indicate that the sacral fibers do not have a direct connection to the sacral bone but instead integrate into the endopelvic fascia.

3.) Regarding the asymmetry of the right and left USL, the current literature only mentions that such asymmetrical conditions exist (31). However, no study provides data comparing the length of the right and the left side or a hypothesis as to why this might be the case.

4.) Although the statistical analysis did not reveal any statistically significant differences in the distribution of smooth muscle, as has been confirmed in other studies (23, 25, 26), a difference in muscle distribution within the USL of individual body donors (regardless of age) could be observed through visual examination of the histological slides under the microscope. The substantial interindividual variability in muscle content, combined with the relatively small sample size compared to other investigations, may account for the absence of statistical significance in our findings.

5.) The difference in the distribution of smooth muscle between the young group and the aged group suggests that the overall proportion of smooth muscle in the USL decreases with age. Since no studies are currently known that examine a correlation between the amount of smooth muscle in the USL and age, this should be investigated further.

4.3. Clinical implications

The insights gained from this study have direct relevance for clinicians, particularly in urogynecology and reconstructive surgery. The regional differences in the USL's fiber

orientation suggest that its mechanical properties are not uniform along its lenght, which could influence surgical outcomes in procedures like uterosacral ligament suspension. Understanding the asymmetrical nature of the USL could help further optimize existing surgical techniques.

Moreover, the findings highlight the potential role of the USL in the pathophysiology of pelvic organ prolapse. Structural degeneration and microstructural changes due to damage in specific regions of the ligament could predispose individuals to developing POP. The observed higher smooth muscle content in the two young women suggest that there could be a decrease of smooth muscle connected to aging. Future therapeutic and surgical approaches may benefit from a deeper understanding of these regional and age-related variations.

4.4. Strengths and limitations

One strength of our study is the use of multiple histological staining techniques enabling a more detailed visualization of connective tissue structures.

Furthermore, due to the lack of a precisely documented method for harvesting the USL from body donations, a standardized extraction technique was successfully developed.

This study demonstrated, that tissue from embalmed body donors initially fixed in formalin and embedded with ethanol can still be effectively utilized for histological staining procedures and subsequent microscopic evaluation and allows comparison with fresh samples. This highlights the potential for using pre-fixed specimens in histological research, which may be particularly valuable in cases where freshly frozen or otherwise untreated tissue is not available.

A limitation of this study is the relatively small sample size, which restricts the generalizability of the findings. Additionally, among the few body donors, no relevant prolapse conditions were examined in any of the women. Therefore, no conclusions could be drawn regarding changes in macro- and microstructure in relation to a previous prolapse but rather changes with healthy aging.

Another limitation of this study was the age of the examined women. As the average age at death was 75 years and only one of the samples were obtained from women under 30, no definitive conclusions but only possible indications could be drawn regarding age-related changes in the microstructure.

4.5. Future directions

Building on these findings, future research should aim to:

- Increase the sample size to include a more diverse population, considering variables such as age, parity, and occurrence of different stages of POP.
- Explore the molecular composition of the USL, focusing on collagen subtypes, elastin, and other extracellular matrix components and their distribution within the USL, and try to connect to biomechanical characteristics.
- Investigate age-related changes in the USL, particularly in the context of postmenopausal tissue remodeling and its implications for POP.
- Conduct biomechanical testing to quantify the tensile strength and elasticity of the USL in different regions, providing direct evidence of its functional capabilities. Samples from the extracted USL have been preserved for future biomechanical testing.

4.6. Conclusion

In conclusion, this study highlights the complex microstructural organization of the uterosacral ligament and its regional specialization in collagen orientation. The observed interindividual variability in the expression of the different components and the varying proportion of smooth muscle across age groups are particularly relevant in the clinical field of gynecology and urogynecology. Surgeries for POP, such as uterosacral ligament fixation or uterosacral hysteropexy, require a certain level of support from the USL's tissue to prevent a recurrent uterine prolapse. The expanded knowledge of the regional structure, indications of age-related changes and an interindividual variability in the USL provide additional information for the further development and optimization of these surgical procedures for the correction of POP.

5. References

1. Deutsche Gesellschaft für Gynäkologie und Geburtshilfe (DGGG), Österreichische Gesellschaft für Gynäkologie und Geburtshilfe (OEGGG), Schweizerische Gesellschaft für Gynäkologie und Geburtshilfe (SGGG). Diagnostik und Therapie des weiblichen Descensus genitalis. 2016

2. AUGS Guidelines. Pelvic Organ Prolapse. Female Pelvic Med Reconstr Surg. 2019 Dec.

3. Vergeldt Tf, Weemhoff M, IntHout J, Kluivers Kb. Risk factors for pelvic organ prolapse and its recurrence: a systematic review. Int Urogynecology J. 2015 Nov.

4. Reay Jones Nh, Healy Jc, King Lj, Saini S, Shousha S, Allen-Mersh Tg. Pelvic connective tissue resilience decreases with vaginal delivery, menopause and uterine prolapse. Br J Surg. 2003 Apr.

5. Ludwig S, Göktepe S, Mallmann P, Jäger W. Evaluation of Different "Tensioning" of Apical Suspension in Women Undergoing Surgery for Prolapse and Urinary Incontinence. Vivo Athens Greece. 2020 Jun.

6. Barber Md, Maher C. Epidemiology and outcome assessment of pelvic organ prolapse. Int Urogynecology J. 2013 Nov.

7. Persu C, Chapple Cr, Cauni V, Gutue S, Geavlete P. Pelvic Organ Prolapse Quantification System (POP-Q) - a new era in pelvic prolapse staging. J Med Life. 2011 Mar.

8. Ellerkmann Rm, Cundiff Gw, Melick Cf, Nihira Ma, Leffler K, Bent Ae. Correlation of symptoms with location and severity of pelvic organ prolapse. Am J Obstet Gynecol. 2001 Dec.

9. Donaldson K, Huntington A, De Vita R. Mechanics of Uterosacral Ligaments: Current Knowledge, Existing Gaps, and Future Directions. Ann Biomed Eng. 2021 Aug.

10. Jelovsek Je, Barber Md. Women seeking treatment for advanced pelvic organ prolapse have decreased body image and quality of life. Am J Obstet Gynecol. 2006 May.

11. Boyles Sh, Weber Am, Meyn L. Procedures for pelvic organ prolapse in the United States, 1979-1997. Am J Obstet Gynecol. 2003 Jan.

12. Bump Rc, Mattiasson A, Bø K, Brubaker Lp, DeLancey Jo, Klarskov P, et al. The standardization of terminology of female pelvic organ prolapse and pelvic floor dysfunction. Am J Obstet Gynecol. 1996 Jul.

13. Pham T, Burgart A, Kenton K, Mueller Er, Brubaker L. Current Use of Pelvic Organ Prolapse Quantification by AUGS and ICS Members. Female Pelvic Med Reconstr Surg. 2011 Mar.

14. Hagen S, Stark D. Conservative prevention and management of pelvic organ prolapse in women. Cochrane Database Syst Rev. 2011 Jul 12.

15. Maher C, Feiner B, Baessler K, Schmid C. Surgical management of pelvic organ prolapse in women. Cochrane Database Syst Rev. 2013 Apr 30.

16. Barber Md. Pelvic organ prolapse. BMJ. 2016 Jul 20.

17. Webb Mj, Aronson Mp, Ferguson Lk, Lee Ra. Posthysterectomy vaginal vault prolapse: primary repair in 693 patients. Obstet Gynecol. 1998 Aug.

18. Miller A, Hong Mk, Hutson Jm. The broad ligament: a review of its anatomy and development in different species and hormonal environments. Clin Anat N Y N. 2004 Apr.

19. Petri E, Ashok K. Sacrospinous vaginal fixation--current status. Acta Obstet Gynecol Scand. 2011 May.

20. Gutman R, Maher C. Uterine-preserving POP surgery. Int Urogynecology J. 2013 Nov.

21. Diwadkar Gb, Barber Md, Feiner B, Maher C, Jelovsek Je. Complication and reoperation rates after apical vaginal prolapse surgical repair: a systematic review. Obstet Gynecol. 2009 Feb.

22. Norton Pa. Pelvic floor disorders: the role of fascia and ligaments. Clin Obstet Gynecol. 1993 Dec.

23. Campbell Rm. The anatomy and histology of the sacrouterine ligaments. Am J Obstet Gynecol. 1950 Jan.

24. Vu D, Haylen Bt, Tse K, Farnsworth A. Surgical anatomy of the uterosacral ligament. Int Urogynecology J. 2010 Sep.

25. Buller Jl, Thompson Jr, Cundiff Gw, Krueger Sullivan L, Schön Ybarra Ma, Bent Ae. Uterosacral ligament: description of anatomic relationships to optimize surgical safety. Obstet Gynecol. 2001 Jun.

26. Iwanaga R, Orlicky Dj, Arnett J, Mk G, Hurt Kj, Connell Ka. Comparative histology of mouse, rat, and human pelvic ligaments. Int Urogynecology J. 2016 Nov.

27. Cole Ee, Leu Pb, Gomelsky A, Revelo P, Shappell H, Scarpero Hm, et al. Histopathological evaluation of the uterosacral ligament: is this a dependable structure for pelvic reconstruction? BJU Int. 2006 Feb.

28. Umek Wh, Morgan Dm, Ashton-Miller Ja, DeLancey Jo. Quantitative analysis of uterosacral ligament origin and insertion points by magnetic resonance imaging. Obstet Gynecol. 2004 Mar.

29. Anton Hafferl. Lehrbuch der Topographischen Anatomie. Walter Thiel, editor. Berlin, Heidelberg: Springer; 1969.

30. Friedrich Anderhuber, Franz Pera, Johannes Streicher. Anatomie des Menschen. 19. Aufl. s.l.: Walter de Gruyter GmbH Co.KG; 2012. 210308 p. (De Gruyter Studium).

31. Ramanah R, Berger Mb, Parratte Bm, DeLancey Jo. Anatomy and histology of apical support: a literature review concerning cardinal and uterosacral ligaments. Int Urogynecology J. 2012 Nov.

32. Ercoli A, Delmas V, Fanfani F, Gadonneix P, Ceccaroni M, Fagotti A, et al. Terminologia Anatomica versus unofficial descriptions and nomenclature of the fasciae and ligaments of the female pelvis: a dissection-based comparative study. Am J Obstet Gynecol. 2005 Oct.

33. Fritsch H, Hötzinger H. Tomographical anatomy of the pelvis, visceral pelvic connective tissue, and its compartments. Clin Anat N Y N. 1995.

34. Siddique Sa, Gutman Re, Schön Ybarra Ma, Rojas F, Handa Vl. Relationship of the uterosacral ligament to the sacral plexus and to the pudendal nerve. Int Urogynecol J Pelvic Floor Dysfunct. 2006 Nov.

35. Connell Ka, Guess Mk, Chen H, Andikyan V, Bercik R, Taylor Hs. HOXA11 is critical for development and maintenance of uterosacral ligaments and deficient in pelvic prolapse. J Clin Invest. 2008 Mar.

36. Han L, Wang L, Wang Q, Li H, Zang H. Association between pelvic organ prolapse and stress urinary incontinence with collagen. Exp Ther Med. 2014 May.

37. Liu C, Wang Y, Li Bs, Yang Q, Tang Jm, Min J, et al. Role of transforming growth factor β-1 in the pathogenesis of pelvic organ prolapse: A potential therapeutic target. Int J Mol Med. 2017 Aug.

38. Yucel N, Usta A, Guzin K, Kanter M, Bilgic E, Ozel No, et al. Immunohistochemical analysis of connective tissue in patients with pelvic organ prolapse. J Mol Histol. 2013 Feb.

39. Zhu Yp, Xie T, Guo T, Sun Zj, Zhu L, Lang Jh. Evaluation of extracellular matrix protein expression and apoptosis in the uterosacral ligaments of patients with or without pelvic organ prolapse. Int Urogynecology J. 2021 Aug.

40. Gabriel B, Denschlag D, Göbel H, Fittkow C, Werner M, Gitsch G, et al. Uterosacral ligament in postmenopausal women with or without pelvic organ prolapse. Int Urogynecol J Pelvic Floor Dysfunct. 2005 Dec.

41. Liapis A, Bakas P, Pafiti A, Frangos-Plemenos M, Arnoyannaki N, Creatsas G. Changes of collagen type III in female patients with genuine stress incontinence and pelvic floor prolapse. Eur J Obstet Gynecol Reprod Biol. 2001 Jul.

42. Goepel C. Differential elastin and tenascin immunolabeling in the uterosacral ligaments in postmenopausal women with and without pelvic organ prolapse. Acta Histochem. 2008.

43. Strinic T, Vulic M, Tomic S, Capkun V, Stipic I, Alujevic I. Matrix metalloproteinases-1, -2 expression in uterosacral ligaments from women with pelvic organ prolapse. Maturitas. 2009 Oct 20.

44. Kökçü A, Yanik F, Cetinkaya M, Alper T, Kandemir B. Histopathological evaluation of the connective tissue of the vaginal fascia and the uterine ligaments in women with and without pelvic relaxation. Arch Gynecol Obstet. 2002 Apr.

45. Schneider CA, Rasband WS, Eliceiri KW. NIH Image to ImageJ: 25 years of image analysis. Nat Methods. 2012 Jul.

46. Landini G, Martinelli G, Piccinini F. Colour deconvolution: stain unmixing in histological imaging. Bioinformatics. 2021 Jun.

Use of AI-Tools

The following tool was used to optimize the language of the text:

ChatGPT-4-turbo, OpenAI

generated on 15.02.2025

https://chatgpt.com

Promt: „Please optimize the language without changing the content."

6. Appendix

1.1. Protocoll of measurements

MESSPROTOKOLL

TISCH NR:

PRÄPARAT NR:

FOTODOKUMENTATION:

Foto ohne Manipulation: O

Foto mit Ventralverlagerung des Uterus: O

BESCHREIBUNG	MESSWERT
äußere Beckenmaße	
Distantia interspinosa	
Distantia intercristalis	
Conjugata externa	
innere Beckenmaße	
Diameter transversa	
Diameter obliqua	
Conjugata anatomica	
Conjugata vera	
Ligamentum sacrouterinum	
Längsausdehnung	
Abstand Insertionsstellen gerade gemessen	
Breite am Sacrum	
Breite im Bereich der Spina ischiadica	
Breite an Cervix/ Vagina	
"Verwachsung" mit CL	

BESONDERHEITEN/ ANMERKUNGEN:

1.2. Protocoll of HE staining

Entparaffinieren / Entwässern	
Xylol 1	10‘
Xylol 2	10‘
100% Ethanol / Xylol 1:1	Kurz
100% Ethanol	Kurz
96% Ethanol	Kurz
80% Ethanol (optional nur in Raum 716)	Kurz
70% Ethanol	Kurz
50% Ethanol (optional nur in Raum 716)	Kurz
Färben	
Hämalaun (n. P. Mayer, selfmade)	10´
Aqua dest.	2-3x, wechseln bis keine Farbe herausgeht
NH3 Wasser 2,5ml Ammoniak/ 1L Aqua dest.	Einige Sekunden/ bis Kerne blau
Aqua dest	Zurück in frisches Aqua dest.
96% Ethanol	Kurz differenzieren bis keine Farbwolken abgehen, verschmutzte Alkohole in den Ausguss, mit Wasser nachschwemmen
100% Ethanol	Kurz
100% Ethanol / Xylol 1:1	Kurz
Xylol 2	Min. 10‘
Eindecken	-

1.3. Protokoll of Sirius-Red-staining

2. Entparaffinieren / Entwässern	
Xylol 1	10‘
Xylol 2	10‘
100% Ethanol / Xylol 1:1	Kurz
100% Ethanol	Kurz
96% Ethanol	Kurz
70% Ethanol	Kurz
Färben	
Aqua nondest.	4´
Weigerts Eisenhämatoxiylin	15‘ (*5% weniger Stammlösung B)
Aqua nondest, fließend	8‘
Aqua dest	1‘
Pikro-Siriusrot	1h
Essigsäure 30%	1‘
Essigsäure 30%	1‘
96% Ethanol	2‘
96% Ethanol	2‘
100% Ethanol	Kurz
100% Ethanol / Xylol 1:1	Kurz
Xylol 2	Min. 10‘
Eindecken	-

2.1. Protocoll of Masson-Goldner-Trichrome staining

3. Entparaffinieren / Entwässern	
Xylol 1	10‘
Xylol 2	10‘
100% Ethanol / Xylol 1:1	Kurz
100% Ethanol	Kurz
96% Ethanol	Kurz
70% Ethanol	Kurz
A. dest.	Kurz
Färben	
Weigerts Eisenhämatoxylin	2‘ (*5% weniger Stammlösung B)
Aqua non dest. (fließend)	10‘
Goldner-Lösung I (Ponceau-Säurefuchsin)	5‘
1% Essigsäure	Spülen
Goldner II (Phosphowolframsäure-Orange G)	5‘
1% Essigsäure	Spülen
Goldner III (Lichtgrün SF)	5‘
Essigsäure 1%	2‘
Waschen in A. dest.	Kurz
96% Ethanol	Kurz
100% Ethanol	Kurz
100% Ethanol / Xylol 1:1	Kurz
Xylol 2	Min. 10‘
Eindecken	-